NASA Contractor Report 178141

LINE SPRING MODEL AND ITS APPLICATIONS TO PART-THROUGH CRACK PROBLEMS IN PLATES AND SHELLS

F. ERDOGAN AND B. AKSEL

LEHIGH UNIVERSITY
BETHLEHEM, PENNSYLVANIA

GRANT NGR 39-007-011
JUNE 1986

NASA
National Aeronautics and
Space Administration
Langley Research Center
Hampton, Virginia 23665

LINE SPRING MODEL AND ITS APPLICATIONS TO PART-THROUGH CRACK PROBLEMS IN PLATES AND SHELLS

by

F. Erdogan[1] and B. Aksel[2]

ABSTRACT: In this paper after giving a general description of the line spring model it is extended to cover the problem of interaction of multiple internal and surface cracks in plates and shells. The shape functions for various related crack geometries obtained from the plane strain solution and the results of some multiple crack problems are presented. The problems considered include coplanar surface cracks on the same or opposite sides of a plate, nonsymmetrically located coplanar internal elliptic cracks, and in a very limited way the surface and corner cracks in a plate of finite width and a surface crack in a cylindrical shell with fixed end.

KEY WORDS: Stress intensity factor, line spring model, surface crack, internal crack, three dimensional crack problem, part-through crack, cracks in plates, cracks in shells.

1. Introduction

The analysis of a part-through crack in a component which may locally be represented by a "plate" or a "shell" is certainly one of the important problems in fracture mechanics. The general problem is one of a three-dimensional crack in a solid with bounded geometry where there is a strong interaction between the stress field disturbed by the crack and the bounding surfaces of the medium. Even under the assumption of linear elasticity a neat analytical treatment of the problem seems to be intractable. The existing solutions, therefore, rely very heavily on the techniques of computational mechanics. In this respect the standard technique has been that of three-dimensional finite element (see, for example, [1]-[5] for some of the typical contributions). Other numerical techniques used have been the boundary integral equation method [6], and the alternating method (see, for example, the article by Shah and Kobayashi in [7]). The finite element and

[1]Professor of Mechanics; [2]Graduate student, Lehigh University, Bethlehem, PA 18015

N86-28468#

the alternating methods have also been combined in a new hybrid technique to treat three dimensional elliptic crack problems [8], [9].

If one is dealing with a relatively thin-walled structure containing a part-through crack in a plane perpendicular to the bounding surfaces of the medium, the three-dimensional crack problem can be made analytically tractable under two important approximating assumptions. The first is the representation of the structure by a "plate" or a "shell" and the second is the treatment of the part-through crack by a "line spring model". Through the use of a plate or a shell theory the coordinate in the thickness direction is suppressed and the basically three-dimensional elasticity problem is rendered two-dimensional. Modeling of the crack by a line spring, on the other hand, not only lends itself to plate or shell treatment but also preserves the basic plane strain character of the stress field along the crack front (everywhere except near the ends). In a relatively thin-walled structure containing a part-through crack the net ligament in the plane of the crack would generally have a constraining effect on the crack opening displacements. The physical concept underlying the line spring model which was first proposed in [10] consists of approximating the three dimensional crack problem by a coupled membrane-bending problem through reducing the net ligament stresses to the neutral axis of the plate or the shell as an (unknown) membrane load N and bending moment M. In the resulting problem the crack surface displacements are also represented by two lumped quantities, namely the crack opening displacement δ and the crack surface rotation θ measured at the neutral surface. The unknowns N, M, δ and θ are now functions of a single variable x_1, the coordinate along the crack in the neutral surface (Fig. 1). The complementary pairs of functions (N,M) and (δ,θ) defined along the crack are not independent and are assumed to be related through the corresponding plane strain problem for the cracked strip. The functions (N,M) or (δ,θ) are determined from the related mixed boundary value problem for the plate or the shell with a through crack in which N and M are treated as unknown crack surface loads. After determining N and M the stress intensity factor at a given location x_1 along the crack is calculated from the corresponding two dimensional elasticity solution of the cracked strip lying in a plane perpendicular to x_1 (Figs. 1c, 2, and 3).

In the original model classical plate bending theory was used and the problem was formulated with N and M as the unknown functions ([10], see also Rice's article in [7]). In the application of the model the main problem is the solution of a plate or a shell containing a through crack and subjected to membrane or bending loads. On the other hand, to have an asymptotic solution around the crack tips in a plate under bending which is compatible with the elasticity results the necessity of using a higher order plate bending theory such as that of Reissner's [11], [12] has now been well-established [13]-[17]. Unlike the classical theory (in which one can use one less boundary condition than needed through the Kirchhoff assumption), the transverse shear theories of plates and shells can accommodate all stress and moment resultants (or their displacement complements) on the crack surfaces separately, that is, one can specify three boundary conditions in plates and five in shells. The consequence of this is that the transverse shear theories give asymptotic results which are identical to those obtained from plane strain and antiplane shear elasticity solutions of the crack problems [16], [17], whereas not only the angular distribution of the stresses given by the classical plate and shell theories are different than the elasticity results, but for skew-symmetric problems even the powers of singularity (in the transverse shear stress) are not in agreement [16]. One may note that compatibility of the asymptotic solutions obtained from the transverse shear theories with the elasticity solutions is not restricted to crack problems. As shown in a recent study [18] the agreement is valid for general wedge-shaped plates of an arbitrary angle.

An additional change introduced into the line spring model as presented in this paper is the use of the "displacements" (δ,θ) rather than the stress and moment resultants (N,M) as the unknown functions in the integral equations. This is simply a matter of convenience, as δ and θ turn out to be more natural unknowns in formulating the problem.

After a period of neglect recently there seems to be a renewed interest in the applications of the model. The reasons for this are that judiciously used the model can give results with acceptable accuracy, requires (comparatively speaking) only nominal computational effort, is highly flexible with regard to crack profile, and, as will be indicated in this paper, can be routinely extended to treat multiple crack problems of varying geometires.

Some recent applications of the model to a variety of plate and shell problems may be found in [19]-[27].

In this paper the line spring model is generalized to cover multiple co-planar cracks of arbitrary orientations including internal as well as the surface cracks and the related stress intensity shape functions are given. The model is applied to plate and shell problems by using Reissner's transverse shear theory and the results of some typical examples are discussed.

2. Description of the Line Spring Model

Let us first consider the problem of a surface crack in a plate or a shell under Mode I loading condition (Fig. 1). Referred to the local coordinate system it will be assumed that u_1, u_2, u_3 are the displacement components, β_1, β_2 are the rotations of the normal to the neutral surface (in, respectively, x_1x_3 and x_2x_3 planes), and N_{ij}, M_{ij}, and V_i, $(i,j=1,2)$ are, respectively, the membrane, bending, and transverse shear resultants. Let N_{22}^{∞} and M_{22}^{∞} be external loads applied to the structure away from the crack region (Fig. 1) and define

$$\sigma_{\infty} = N_{22}/h \ , \ m_{\infty} = 6M_{22}^{\infty}/h^2 \ . \tag{1}$$

Similarly, let N and M represent membrane and bending resultants statically equivalent to the net ligament stress $\sigma_{22}(x_1,0,x_3)$ (Fig. 1c) and define

$$\sigma(x_1) = N(x_1,0)/h \ , \ m(x_1) = 6M(x_1,0)/h^2 \ . \tag{2}$$

Defining now the unknown functions

$$f_1(x_1) = \frac{\partial}{\partial x_1} \beta_2(x_1,+0) \ , \ f_2(x_1) = \frac{\partial}{\partial x_1} u_2(x_1,+0) \ , \tag{3}$$

and referring to, for example, [24] and [17] for details, the through crack problem for the structure under the applied loads (1) and (2) may be expressed as

$$\sum_1^2 \int_{-a}^{a} k_{ij}(x_1,t)f_j(t)dt = g_i(x_1) \ , \ (-a<x_1<a, \ i=1,2) \ , \tag{4}$$

$$\int_{-a}^{a} f_j(t)dt = 0, \ (j=1,2) \ , \tag{5}$$

where

$$g_1(x_1) = [-m_\infty + m(x_1)]/6E \ , \ g_2(x_1) = [-\sigma_\infty + \sigma(x_1)]/E \ . \tag{6}$$

In shells the integral equations (4) are coupled (i.e., k_{12} and k_{21} are nonzero), whereas in plates bending-membrane coupling would be through the input functions m and σ only. Note that m and σ tend to close the crack surfaces while the external loads m_∞ and σ_∞ tend to open them.

The first approximating assumption made in developing the line spring model is that the crack is a through crack and the constraint caused by the net ligament stress $\sigma_{22}(x_1,0,x_3)$ tending to prevent the crack from opening and rotating may be accounted for by applying the membrane and bending resultants N and M on the crack surfaces. The second major assumption states that the stress intensity factor along the crack front at a location x_1 may be approximated by the corresponding plane strain value obtained from a strip which contains a part-through crack of length $L(x_1)$ and is subjected to uniform tension $N(x_1)$ and bending $M(x_1)$ away from the crack region (Figs. 1 and 2). The main problem in the development of the model is expressing the functions N and M in terms of the unknown functions f_1 and f_2 and it is the second assumption which makes this possible.

To obtain N and M in terms of f_1 and f_2 we now express the energy available for fracture in two alternate forms. First we note that at a location x_1 along the crack front by using the crack closure concept the energy available for fracture may be expressed as

$$G = \frac{\partial}{\partial L}\,(U-V) = \frac{1-\nu^2}{E}\,K_1{}^2 \tag{7}$$

where $L(x_1)$ is the crack size, K_1 is the stress intensity factor, U is the work done by the external loads, V is the strain energy, and E and ν are the elastic constants. From the solution of the plane elasticity problem the stress intensity factor for an edge crack shown in Fig. 2 is obtained as follows:

$$K_1 = \sqrt{h}\,[\sigma g_t(s) + m g_b(s)] \ , \ s = L/h \tag{8}$$

where σ and m are given by (2). For analytical convenience the shape functions g_t and g_b may be expressed as

$$g_t(s) = \sqrt{\pi s}\ \sum_{0}^{6}\ b_i s^{2i}\ ,\ g_b(s) = \sqrt{\pi s}\ \sum_{0}^{6} c_i s^i\ ,\ s=L/h\ . \qquad (9)$$

The calculated values(*) of K_1 and the coefficients b_i and c_i obtained from a least square curve fit are given in Table 1.

Referring to Fig. 2, we now let $d\delta$ and $d\theta$ be the changes in the "load line displacements" δ and θ (corresponding to "loads" N and M) as the crack length goes from L to L+dL under "fixed load" conditions. From Fig. 2b it then follows that

$$dU = Nd\delta + Md\theta \qquad (10)$$

$$dV = \frac{1}{2}[N(\delta+d\delta)+M(\theta+d\theta)] - \frac{1}{2}\ (N\delta+M\theta) = \frac{1}{2}(Nd\delta+Md\theta)\ , \qquad (11)$$

giving the energy available for crack growth dL as

$$d(U-V) = \frac{1}{2}\ (Nd\delta+Md\theta)\ . \qquad (12)$$

Observing that for constant N and M and varying L

$$d\delta = \frac{\partial\delta}{\partial L}\,dL\ ,\ d\theta = \frac{\partial\theta}{\partial L}\,dL\ , \qquad (13)$$

from (12), (13) and (7) we obtain

$$\frac{\partial}{\partial L}\ (U-V) = \mathcal{G} = \frac{1}{2}\ (N\ \frac{\partial\delta}{\partial L} + M\ \frac{\partial\theta}{\partial L}) = \frac{1-\nu^2}{E}\ K_1{}^2\ . \qquad (14)$$

If we now define the matrices

$$\tau = (\tau_i) = \begin{bmatrix} m \\ \sigma \end{bmatrix}\ ,\ \omega = (\omega_i) = \begin{bmatrix} h\theta/6 \\ \delta \end{bmatrix}\ ,\ G(s) = (g_{ij}) = \begin{bmatrix} g_b{}^2 & g_b g_t \\ g_b g_t & g_t{}^2 \end{bmatrix}\ , \qquad (15)$$

substituting from (2) and (8) into (14) we obtain

$$\mathcal{G} = (\frac{1-\nu^2}{E}\ h)\tau^T G\tau = (\frac{h}{2})\ \tau^T\ \frac{\partial\omega}{\partial L}\ , \qquad (16)$$

giving

(*) The values of K, shown in Table 1, are from [28] and are considered to be accurate.

$$\frac{\partial\omega}{\partial L} = \frac{2(1-\nu^2)}{E} G\tau \ . \tag{17}$$

Note that G is a function and τ is independent of the variable L and $\omega=0$ for L=0. Thus, from (17) it is seen that

$$\omega = \frac{2(1-\nu^2)}{E} \left(\int_0^L G dL\right)\tau \quad . \tag{18}$$

Referring to (3), (5) and Fig. 2, if we observe that

$$\delta = 2u_2(x_1,0) = 2\int_{-a}^{x_1} f_2(t)dt, \ \theta = 2\beta_2(x_1,0) = 2\int_{-a}^{x_1} f_1(t)dt \ , \tag{19}$$

equation (18) gives the desired relationship between the pairs of complementary quantities (m,σ) and (f_1,f_2) which may be expressed as

$$\tau = \begin{bmatrix} m \\ \sigma \end{bmatrix} = \frac{E}{1-\nu^2}\left(\int_0^L G dL\right)^{-1} \begin{bmatrix} \frac{h}{6}\int_{-a}^{x_1} f_1(t)dt \\ \int_{-a}^{x_1} f_2(t)dt \end{bmatrix} \ . \tag{20}$$

It should also be observed that since the crack depth $L(x_1)$ is a known function of x_1, the coefficient matrix C defined by

$$C = (c_{ij}(x_1)) = \frac{1}{1-\nu^2}\left(\int_0^L G dL\right)^{-1} \tag{21}$$

would also consist of known functions $c_{ij}(x_1)$ of x_1.

Substituting now from (20) and (21) into (4) and rearranging, we obtain

$$\int_{-a}^{a} [k_{11}(x_1,t)f_1(t)+k_{12}(x_1,t)f_2(t)]dt - \frac{h}{36} c_{11}(x_1)\int_{-a}^{x_1} f_1(t)dt$$

$$- \frac{1}{6} c_{12}(x_1)\int_{-a}^{x_1} f_2(t)dt = -\frac{m_\infty}{6E} \ , \ (-a<x_1<a) \ ,$$

$$\int_{-a}^{a} [k_{21}(x_1,t)f_1(t)+k_{22}(x_1,t)f_2(t)]dt - \frac{h}{6} c_{21}(x_1)\int_{-a}^{x_1} f_1(t)dt$$

$$- c_{22}(x_1)\int_{-a}^{x_1} f_2(t)dt = -\frac{\sigma_\infty}{E} \ , \ (-a<x_1<a) \ . \tag{22a,b}$$

After solving (22) for f_1 and f_2 the stress intensity factor $K_1(x)$ may be obtained from (20) and (8).

If the plate or the shell contains collinear surface cracks in x_1x_3 plane along $a_k<x_1<b_k$, $(k=1,\ldots,n)$, the integral equations (8) remain essentially unchanged and the problem can be solved by defining the unknown functions f_1 and f_2 given by (3) for each crack separately.

3. Internal and Multiple Cracks

The line spring model described in the previous section can be applied to any coplanar part-through crack problem provided on any cross-section parallel to the x_2x_3 plane there is only one net ligament and one crack, if any (Figs. 1c and 2). The model can also be extended to apply to part-through cracks involving more than one net ligament as in internal cracks (Fig. 3) or more than one crack as in coplanar surface cracks on both sides of the plate or the shell. Here the major difficulty lies in the fact that in such cases usually there is more than one stress intensity factor that must be expressed in terms of more than one dimensionless variable. Thus, aside from the generalization of the basic concept, the problem reduces to sufficiently accurate parametrization of the stress intensity factors.

Consider, for example, the nonsymmetric crack geometry shown in Fig. 3. The integral equations for the corresponding through crack problem is again given by (8). The difference between the two problems is in expressing the resultants $\sigma(x_1)$ and $m(x_1)$ in terms of the unknown functions f_1 and f_2 defined by (3). At each cross-section we note that there are two dimensionless length parameters, $L(x_1)/h$ and $d(x_1)/h$. The problem can be, however, simplified quite considerably if we restrict the discussion to cracks which are symmetric with respect to $x_3=d$ plane (Fig. 3). Thus, defining the plane internal crack by

$$-a<x_1<a,\ x_2=0,\ d-\frac{L(x_1)}{2} < x_3 < d+\frac{L(x_1)}{2}\ , \tag{23}$$

in the discussion that follows it will be assumed that d is independent of x_1. Referring to Fig. 3b, if K_A and K_B are the stress intensity factors at the crack tips A and B obtained from the plane elasticity solution, for an increase dL in the crack length the energy increment available for fracture (as determined from crack closure) may be expressed as

$$d(U-V) = \frac{1-\nu^2}{E}\left[K_A^2 \frac{dL}{2} + K_B^2 \frac{dL}{2}\right] , \tag{24}$$

or

$$G = \frac{\partial}{\partial L}(U-V) = \frac{1-\nu^2}{2E}(K_A^2+K_B^2) . \tag{25}$$

We now note that as long as there is only one variable L representing the crack size, the argument leading to the expression of G in terms of (N,M) and (δ,θ) will remain unchanged (see eqs. (10)-(14)) and from (14) and (25) it follows that

$$\frac{1}{2}\left(N \frac{\partial\delta}{\partial L} + M \frac{\partial\theta}{\partial L}\right) = \frac{1-\nu^2}{2E}(K_A^2+K_B^2) . \tag{26}$$

The solution of the plane elasticity problem shown in Fig. 3b is available [29] and K_A and K_B can be expressed in terms of certain shape functions as follows:

$$\begin{aligned} K_A &= \sqrt{h}\,[\sigma g_{At}(s) + m g_{Ab}(s)] , \\ K_B &= \sqrt{h}\,[\sigma g_{Bt}(s) + m g_{Bb}(s)] , \\ s &= L/h,\ \sigma = N/h,\ m = 6M/h^2 . \end{aligned} \tag{27}$$

The shape functions are, in turn, expressed by

$$\begin{aligned} g_{At}(s) &= \sqrt{\pi s}\sum_{i=D}^{n} b_{Ai}s^{2i} , \quad g_{Ab}(s) = \sqrt{\pi s}\sum_{0}^{n} c_{Ai}s^{i} , \\ g_{Bt}(s) &= \sqrt{\pi s}\sum_{0}^{n} b_{Bi}s^{2i} , \quad g_{Bb}(s) = \sqrt{\pi s}\sum_{0}^{n} c_{Bi}s^{i} , \quad s = L/h , \end{aligned} \tag{28a-d}$$

where for a given d the coefficients are obtained from [29] by using a least square curve fit [30].

For d=0, $K_A=K_B$ in tension and $K_A=-K_B$ in bending and the corresponding membrane and bending stress intensity factors as well as the coefficients b_i and c_i are given in Table 2 [30]. In the case of nonsymmetrically located internal crack, for six different values of d/h the coefficients of the shape functions as defined by (28) are shown in Table 3 [30].

By examining the equations (14) through (22), from the derivation given in the previous section it may be seen that the only difference between the models representing the surface crack and the internal crack will be in the matrix G(s) defined by (15) for the edge crack. In particular for the internal crack problem (20) will remain valid provided the matrix G is evaluated from

$$G(s) = \frac{1}{2}\begin{bmatrix} g_{Ab}^2+g_{Bb}^2 & g_{Ab}g_{At}+g_{Bb}g_{Bt} \\ g_{Ab}g_{At}+g_{Bb}g_{bt} & g_{At}^2+g_{Bt}^2 \end{bmatrix} \tag{29}$$

which follows from (26)-(28) and (16).

Another special case is that of two coplanar surface cracks symmetrically located on the opposite sides of the plate (Fig. 4). Going through the argument step by step one may easily show that, except for the shape functions, this case is identical to the internal crack problem with d=0 (Fig. 3). If the plate is under membrane loading only, because of symmetry no bending would take place and there is no need for the bending components of the shape functions, g_{Ab}, g_{Bb}. For the corresponding symmetric edge cracks of depths L/2 the stress intensity factors and the coefficients b_i for the membrane shape function are given in Table 4 [30].

For more general crack geometries the problem can be rather complicated. Consider, for example, the nonsymmetric case of the surface crack problem shown in Fig. 4. Let the two cracks be defined by reasonably smooth arbitrary functions $L_1(x_1)$ and $L_2(x_1)$ and again designate the crack tips at an x_1 = constant plane by A and B (corresponding to cracks L_1 and L_2, respectively). The energy available for incremental crack growths dL_1 and dL_2 may again be expressed in the following alternate forms:

$$d(U-V) = \frac{1-\nu^2}{E}\,[K_A^2 dL_1 + K_B^2 dL_2] \,, \tag{30}$$

$$d(U-V) = \frac{1}{2}[(N\frac{\partial\delta}{\partial L_1} + M\frac{\partial\theta}{\partial L_1})dL_1 + (N\frac{\partial\delta}{\partial L_2} + M\frac{\partial\theta}{\partial L_2})dL_2] \;. \tag{31}$$

If we now define the matrices as in (15) replacing G by G_A and G_B (where the shape functions as defined in (27) would be functions of the variables $s_1=L_1/h$ and $s_2=L_2/h$), from (30) and (31) it can be shown that

$$\frac{\partial\omega}{\partial L_1}\,dL_1+\frac{\partial\omega}{\partial L_2}\,dL_2 = d\omega = \frac{2(1-\nu^2)}{E}\,(G_A dL_1+G_B dL_2)\tau \tag{32}$$

Again by observing that $\omega=0$ for $L_1=0=L_2$ and $L_1=L_1(x_1)$, $L_2=L_2(x_1)$, from (32) we find

$$\omega(x_1) = \frac{2(1-\nu^2)}{E}\,\left(\int_0^{L_1} G_A dL_1 + \int_0^{L_2} G_B dL_2\right)\tau \quad . \tag{33}$$

From (33) and (18)-(21) it then follows that the integral equations (22) are still valid provided the matrix C defined by (21) is replaced by

$$C = (c_{ij}(x_1)) = \frac{1}{2(1-\nu^2)}\,\left(\int_0^{L_1} G_A dL_1 + \int_0^{L_2} G_B dL_2\right)^{-1} \quad . \tag{34}$$

Of course the main difficulty in problems such as the one described above is that they require a complete two-way parametrization of the stress intensity factors or the determination of the shape functions $g_{\alpha\beta}$ ($\alpha=(A,B)$, $\beta=(t,b)$) as functions of two variables $s_1=L_1/h$ and $s_2=L_2/h$.

4. Applications and Some Results

In order to apply the line spring model to coplanar multiple cracks the integral equations need to be cast in a more convenient form. First we note that for the case of through cracks in plates and shells derivation of the integral equations for collinear multiple cracks is no more difficult than for a single crack. In fact, if no symmetry with respect to the coordinate x_1 is required (Fig. 1), the expressions of the kernels for the two cases are identical. If, for example, the structure contains P through cracks in x_1x_3 plane along $a_p<x_1<b_p$, $p=1,2,\ldots,P$, the integral equations for a plate or a shallow shell (replacing (4) and (5)) may be expressed as

$$\sum_{p=1}^{P}\int_{a_p}^{b_p}\sum_{1}^{2} k_{ij}(x_1,t)f_j(t)dt = g_i(x_1) \ , \ x_1 \in \sum_{1}^{P}(a_p,b_p) \ , \tag{35}$$

$$\int_{a_p}^{b_p} f_j(t)dt = 0,\ j = 1,2,\ p = 1,\ldots,P \ , \tag{36}$$

where the functions g_i again represent the crack surface loads and in the case of part-through cracks the definitions given by (3), (6), (1) and (2) are still valid. We note that there are really 2P unknown functions in the problem, namely f_1 and f_2 on each one of the P cracks. Thus, for the purpose of solving the integral equations, (35) can be written in a more convenient form by defining

$$f_i(x_1) = f_{ip}(x_1),\ a_p<x_1<b_p,\ p=1,\dots,P,\ i=1,2, \tag{37}$$

$$m(x_1) = m_p(x_1),\ a_p<x_1<b_p,\ p=1,\dots,P, \tag{38}$$

$$\sigma(x_1) = \sigma_p(x_1),\ a_p<x_1<b_p,\ p=1,\dots,P\ . \tag{39}$$

We also observe that for each crack the net ligament resultants m and σ are related to f_1 and f_2 through equations such as (20) and (21) where the matrices G and C are dependent on the local (two dimensional) crack geometry and C is a function of x_1. This means that, using (21), (20) may be replaced by

$$\tau_p = \begin{bmatrix} m_p \\ \sigma_p \end{bmatrix} = EC^p_{(x_1)} \begin{bmatrix} \frac{h}{6}\int_{a_p}^{x_1} f_{1p}(t)dt \\ \int_{a_p}^{x_1} f_{2p}(t)dt \end{bmatrix},\ a_p<x_1<b_p,\ p=1,\dots,P. \tag{40}$$

If we now express the integral equations for each interval (a_p,b_p) separately, from (35)-(40) and (6) we obtain

$$\sum_{p=1}^{P}\int_{a_p}^{b_p}\sum_{j=1}^{2} k_{1j}(x_1,t)f_{jp}(t)dt - \frac{h}{36}c^r_{11}(x_1)\int_{a_r}^{x_1} f_{1r}(t)dt$$

$$- \frac{1}{6}c^r_{12}(x_1)\int_{a_r}^{x_1} f_{2r}(t)dt = -\frac{m_\infty}{6E},\ (a_r<x_1<b_r,\ r=1,\dots,P)\ , \tag{41}$$

$$\sum_{p=1}^{P}\int_{a_p}^{b_p}\sum_{j=1}^{2} k_{2j}(x_1,t)f_{jp}(t)dt - \frac{h}{6}\, c_{21}^{r}(x_1)\int_{a_r}^{x_1} f_{1r}(t)dt$$

$$- c_{22}^{r}(x_1)\int_{a_r}^{x_1} f_{2r}(t)dt = -\frac{\sigma_\infty}{E}\ , \ (a_r<x_1<b_r,\ r=1,\dots,P)\ , \tag{42}$$

$$\int_{a_r}^{b_r} f_{ir}(t)dt = 0,\ (i=1,2,\ r=1,2,\dots,P)\ , \tag{43}$$

where the functions $c_{ij}^{r}(x_1)$ are determined from (21) or (34) by using the geometry and the shape functions for the rth crack.

It is seen that once the kernels k_{ij} corresponding to the through cracks are determined and the part through crack profiles $L_r(x_1)$ (or L_{r1} and L_{r2}) are specified, the integral equations (41) and (42) (subject to conditions (43)) may be solved for $f_{jr}(t)$ and equations (40) and (8) or (27) would then give the stress intensity factors as functions of x_1. The kernels k_{ij} for various plates and shells containing through cracks may be found in [21], [22], [24]-[26]. For example, if we use a length parameter a^* (usually a half crack length) to normalize the dimensions, coordinates, and other quantities as

$$x_1/a^* = x,\ u_2/a^* = v,\ a_p/a^* = a_p',\ b_p/a^* = b_p' \tag{44}$$

and define

$$\frac{\partial}{\partial x}\,\beta_2(x,+0) = \phi_1(x)\ ,\ \frac{\partial}{\partial x}\,v(x,+0) = \phi_2(x)\ , \tag{45}$$

The integral equations (35) for an infinite plate may be expressed as [31]

$$\frac{h}{24\pi a^*}\sum_{1}^{P}\int_{a_p'}^{b_p'}\left\{\frac{3+\nu}{1+\nu}\,\frac{1}{\xi-x} - \frac{4h^2}{5(a^*)^2(1+\nu)}\,\frac{1}{(\xi-x)^3} + \frac{4}{1+\nu}\,\frac{1}{\xi-x}\,K_2(\gamma|\xi-x|)\right\}\phi_1(\xi)d\xi$$

$$= -\frac{m_\infty}{6E} + \frac{m(x)}{6E}\ ,\ x\in\sum_{1}^{P}(a_p',b_p')\ , \tag{46}$$

$$\frac{1}{\pi}\sum_{1}^{P}\int_{a_p'}^{b_p'}\frac{\phi_2(\xi)}{\xi-x}\,d\xi = \frac{2}{E}\,[-\sigma_\infty+\sigma(x)],\quad x\in\sum_{1}^{P}(a_p',b_p')\ , \tag{47}$$

where $\gamma = 10(a^*)^2/h^2$.

To give an idea about the applications of the line spring model some sample results are shown in Tables 5-10 and in Figures 6-13. Table 5 gives the normalized stress intensity factor at the deepest penetration points of two coplanar semielliptic surface cracks symmetrically located on the opposite sides of an infinite plate under uniform tension σ_0=N/h (Fig. 4). The table also shows the corresponding plane strain result which is the limiting value of the stress intensity factor as the crack length 2a tends to infinity. In this as well as in other examples discussed in this section the crack border in x_1x_3 plane is assumed to be defined by (Fig. 1)

$$L(x_1) = L_0\sqrt{1-x_1^2/a^2} \tag{48}$$

where a is the half crack length.

The results for the two semi-elliptic coplanar surface cracks of same dimensions and located on the same side of an infinite plate are given in Tables 6 and 7. Table 6 shows the maximum value of the normalized stress intensity factor for the plate under uniform tension σ_0 in a direction perpendicular to the plane of the crack. The notation used in these tables regarding the dimensions is the same as in Fig. 5a with d=h/2. The stress intensity factor for the same plate under bending is given in Table 7. The tables also show the stress intensity factors for the single surface crack which are the limiting values of the two crack results for $b\to\infty$. In the two crack problem considered the distribution of stress intensity factor $K(x_1)$ along the crack border (or as a function of x_1) is somewhat skewed and the maximum K occurs at a value of x_1 that is somewhat less than b+a [24].

Figure 6 shows the normalized stress intensity factor in a plate containing a symmetrically located internal elliptic crack (d=0, Fig. 3) at the points where the minor axis intersects the crack border. The results are given for a plate under uniform tension perpendicular to the plane of the crack. In this as well as in the symmetric surface crack problem considered in Table 5 there is no bending and hence the solution by the line spring method is extremely simple. The figure also shows the finite element results from [3]. Disregarding some small values of a/L_0 for which the line spring model is not really suitable, it may be noted that the agreement between the two results is fairly good.

Some sample results for an excentrically located internal elliptic crack are shown in Figures 7-10. K_A and K_B shown in these figures correspond to the points at the midsection of the ellipse (see the insert in Fig. 7). Figures 7 and 8 show the normalized stress intensity factors in a plate under uniform tension σ_0 for a fixed value of $a/L_0=4$ and varying values of d/h and L_0/h. Figures 9 and 10 show the tension results for $d/h = 0.15$ and varying values of L_0/h and a/L_0.

The normalized stress intensity factor for two symmetrically located identical coplanar internal elliptic cracks in a plate under uniform tension is given in Table 8 (d=0, Fig. 5a). The table shows the results at the midsection of the ellipses. The result for the limiting case of a single crack is also given in the table.

The results for three identical cracks shown in Fig. 5b are given in Table 9. In this case, too, K_A and K_B refer to the points of intersection of the minor axes of ellipses with the crack border (Fig. 5b). Since $d\neq0$ K_A and K_B are not equal. One may observe that the stress intensity factors for the middle crack are only slightly higher than that for the two end cracks. If one may make one general observation regarding the interaction between multiple cracks, it would be that for the same crack lengths and distances in x_1 direction, the interaction for the part-through cracks is much weaker than the interaction between through cracks.

An example for the distribution of the stress intensity factors along the crack border is given in Table 10. More extensive results on the interaction of multiple part-through cracks of various geometries in an infinite plate may be found in [30].

Some results for a plate of finite width are shown in Figures 11 and 12. Fig. 11 shows the distribution of the normalized stress intensity factors for a symmetrically located surface crack having a semi-elliptic or a rectangular profile. The normalizing stress intensity factors shown in these figures are the corresponding plane strain values for an edge-cracked strip and are defined by (see equations 8 and 9)

$$K_{to} = \frac{N_{22}^{\infty}}{h} \sqrt{h}\, g_t(s_o) \ , \ K_{bo} = \frac{6M_{22}^{\infty}}{h^2} \sqrt{h}\, g_b(s_o), \ s_o = L_o/h \ . \tag{49}$$

Figure 12 shows an example for the corner cracks. More extensive results for multiple cracks in a plate of finite width obtained by using the line spring model and comparison with some of the finite element solutions may be found in [24].

Aside from some additional rather complicated Fredholm kernels in the integral equations for shells, from a viewpoint of applications of the line spring model, the problems in shells and plates are identical. The results for various crack and shell geometries obtained by using a transverse shear theory of shallow shells are given in [22], [23], [25] and [26]. Figure 13 shows an example for a pressurized cylindrical shell with a fixed end containing a semi-elliptic axial surface crack. The problem may simulate a rigid end plate or a relatively heavy flange. It is seen that the effect of shell curvature on the stress intensity factors can be very significant.

In reviewing the results one may conclude that, despite its simplicity, carefully and judiciously applied, the line spring model may give very useful results for some three-dimensional part-through crack problems that are otherwise analytically intractable. The method is naturally suited to account for plastic deformations in certain approximate ways. The questions currently being studied concern the extension of the model to mixed-mode problems where, unlike the Mode I case, Modes II and III are always coupled.

Acknowledgement. The work reported in this paper was supported by NASA-Langley under the Grant NGR 39007011 and by NSF under the Grant MEA-8414477.

5. References

1. Raju, I.S. and Newman, Jr., J.C. "Stress Intensity Factors for a Wide Range of Semi-elliptical Surface Cracks in Finite Thickness Plates", J. Engng. Fracture Mechanics, Vol. 11, pp. 817-829, 1979.

2. Newman, Jr., J.C. and Raju, I.S. "Stress Intensity Factors for Internal Surface Cracks in Cylindrical Pressure Vessels", NASA Technical Memorandum 88073, July 1979, (see also ASME J. of Pressure Vessel Technology, Vol. 102, pp. 342-346, 1980).

3. Newman, Jr., J.C. and Raju, I.S. "Stress Intensity Factor Equations for Surface Cracks in Three-Dimensional Finite Bodies", ASTM, STP-791; 1983.

4. McGowan, J.J. and Raymond, M. "Stress Intensity Factor Solutions for Internal Longitudinal Semi-elliptic Surface Flaws in a Cylinder under Arbitrary Loading", Fracture Mechanics, ASTM-STP 677, 1979.

5. Atluri, S.N. and Kathiresan, "3-D Analysis of Surface Flaws in Thick-Walled Reactor Pressure Vessels Using Displacement-Hybrid Finite Element Method", Nuclear Engineering and Design, Vol. 51, pp. 163-176, 1980.

6. Heliot, J., Labbens, R.C. and Pellissier-Tanon, A. "Semi-elliptic Cracks in the Meridional Plane of a Cylinder Subjected to Stress Gradients", Fracture Mechanics, ASTM-STP 677, 1979.

7. The Surface Crack: Physical Problems and Computational Solutions, J.L. Swedlow, ed. ASME, New York, 1972.

8. Nishioka, T. and Atluri, S.N. "Analytical Solution for Embedded Elliptical Cracks and Finite Element Alternating Method for Elliptical Surface Cracks Subjected to Arbitrary Loadings", Engineering Fracture Mechanics, Vol. 17, pp. 247-268, 1983.

9. Nishioka, T. and Atluri, S.N. "Analysis of Surface Flaws in Pressure Vessels by a New 3-D Alternating Method" ASME Journal of Pressure Vessel Technology, Vol. 104, pp. 299-307, 1982.

10. Rice, J.R. and Levy, N. "The Part-through Surface Crack in an Elastic Plate", J. Appl. Mech., Vol. 39, Trans. ASME, pp. 185-194, 1972.

11. Reissner, E. "On Bending of Elastic Plates", Quarterly of Applied Mathematics, Vol. 5, p. 55, 1947.

12. Reissner, E. and Wan, F.Y.M. "On the Equations of Linear Shallow Shell Theory", Studies in Applied Mathematics, Vol. 48, p. 132, 1969.

13. Knowles, J.K. and Wang, N.M. "On the Bending of an Elastic Plate Containing a Crack", J. of Mathematics and Physics, Vol. 39, p. 223, 1960.

14. Wang, N.M. "Effects of Plate Thickness on the Bending of an Elastic Plate Containing a Crack", J. of Mathematics and Physics, Vol. 47, p. 371, 1968.

15. Hartranft, R.J. and Sih, G.C. "Effect of Plate Thickness on the Bending Stress Distribution around Through Cracks", J. of Mathematics and Physics, Vol. 47, p. 276, 1968.

16. Delale, F. and Erdogan, F. "The Effect of Transverse Shear in a Cracked Plate under Skewsymmetric Loading", J. Appl. Mech., Vol. 46, Trans. ASME, pp. 618-624, 1979.

17. Delale, F. and Erdogan, F. "Transverse Shear Effect in a Circumferentially Cracked Cylindrical Shell", Quarterly of Applied Mathematics, Vol. 37 p. 239, 1979.

18. Burton, W.S. and Sinclair, G.B. "On the Singularities in Reissner's Theory for Bending of Elastic Plates", J. of Applied Mechanics, Vol. 53 pp. 220-222, Trans. ASME, 1986.

19. Parks, D.M. "The Inelastic Line Spring: Estimates of Elastic-plastic Fracture Parameters for Surface Cracked Plates and Shells", Paper 80-C2/PVP-109, ASME, 1980.

20. Parks, D.M. "Inelastic Analysis of Surface Flaws Using the Line Spring Model", Proceedings of the 5th Int. Conf. on Fracture, Cannes, France, 1981.

21. Delale, F. and Erdogan, F. "Line Spring Model for Surface Cracks in a Reissner Plate", Int. J. Engng. Sci., Vol. 19, p. 1331, 1981.

22. Delale, F. and Erdogan, F. "Application of the Line Spring Model to a Cylindrical Shell Containing a Circumferential or an Axial Part-through Crack", J. Appl. Mech., Vol. 49, p. 97, Trans. ASME, 1982.

23. Erdogan, F. and Ezzat, H. "Fracture of Pipelines Containing a Circumferential Crack", Welding Research Council Bulletin 288, WRC, 1983.

24. Erdogan, F. and Boduroglu, H. "Surface Cracks in a Plate of Finite Width under Extension or Bending", Theoretical and Applied Fracture Mechanics, Vol. 2, pp. 197-216, 1984.

25. Erdogan, F. and Yahsi, O.S. "A Cylindrical Shell with a Stress-Free End Which Contains an Axial Part-through or Through Crack", Int. J. Engng. Sci., Vol. 23, pp. 1215-1237, 1985.

26. Yahsi, O.S. and Erdogan, F. "A Pressurized Cylindrical Shell with a Fixed End Which Contains an Axial Part-through or Through Crack", Int. J. of Fracture, Vol. 28, pp. 161-187, 1975.

27. Alabi , J.A. and Sanders, Jr., J.L. "Circumferential Part-through Cracks in Cylindrical Shells Under Tension", Journal of Applied Mechanics, Vol. 52, Trans. ASME, pp. 478-479, 1985.

28. Kaya, A.C. and Erdogan, F. "On the Solution of Integral Equations with Strongly Singular Kernels" (to appear in the Quarterly of Applied Mathematics, 1987), NASA CR-178138, June 1986.

29. Kaya, A.C. and Erdogan, F. "Stress Intensity Factors and COD in an Orthotropic Strip", Int. Journal of Fracture, Vol. 16, pp. 171, 1980.

30. Aksel, B. and Erdogan, F. "Interaction of Part-Through Cracks in a Flat Plate", NASA CR-177926, April 1985.

31. Boduroglu, H. and Erdogan, F. "Internal and Edge Cracks in a Plate of Finite Width Under Bending", J. Appl. Mech., Vol. 50, pp. 621-629, Trans. ASME, 1983.

Table 1. The stress intensity factors and the coefficients b_i and c_i of the shape functions $g_t(s)$ and $g_b(s)$ in a strip containing an edge crack of length L and subjected to uniform tensile stress N/h and bending moment M (see eqs. 8 and 9 and Fig. 2).

L/h	Tension $K_1/(N/h)\sqrt{\pi L}$	Bending $K_1/(6M/h^2)\sqrt{\pi L}$	b_i	c_i	i
$\to 0$	1.12152226	1.12152226	1.1215	1.1202	0
10^{-5}	1.121522	1.1215	6.5200	-1.8872	1
10^{-3}	1.121531	1.1202	-12.3877	18.0143	2
0.1	1.1892	1.0472	89.0554	-87.3851	3
0.2	1.3673	1.0553	-188.6080	241.9124	4
0.3	1.6599	1.1241	207.3870	-319.9402	5
0.4	2.1114	1.2606	-32.0524	168.0105	6
0.5	2.8246	1.4972			
0.6	4.0332	1.9140			
0.7	6.3549	2.7252			
0.8	11.955	4.6764			
0.85	18.628	6.9817			
0.9	34.633	12.462			
0.95	99.14	34.31			

Table 2. The stress intensity factors and the coefficients of shape functions in a strip with a symmetric internal crack (d=0, Fig. 3b) under tension and bending (see eqs. 27 and 28).

L/h	Tension $K_A/\sigma\sqrt{\pi L/2}$	Bending $K_A/m\sqrt{\pi L/2}$	$b_{Ai}=b_{Bi}$	$c_{Ai}=c_{Bi}$	i
0.05	1.0002	0.0250	0.7071	0.1013	0
0.1	1.0060	0.0500	0.4325	-0.4629	1
0.2	1.0246	0.1001	-0.1091	15.0622	2
0.3	1.0577	0.1505	7.3711	-143.7384	3
0.4	1.1094	0.2023	-57.7894	807.2449	4
0.5	1.1867	0.2573	271.1551	-2844.8525	5
0.6	1.3033	0.3197	-744.4204	6468.9152	6
0.7	1.4884	0.3986	1183.9529	-9477.5512	7
0.8	1.8169	0.5186	-1001.4920	8638.7826	8
0.9	2.585	0.7776	347.9786	-4455.2167	9
0.95	4.252	1.1421	347.9786	5959.4888	10

Table 3. Coefficients of the shape functions in a strip with an asymmetric internal crack under tension and bending; d≠0, see eqs. (27) and (28) and Fib. 3b.

d/h	i	b_{Ai}	b_{Bi}	c_{Ai}	c_{Bi}
0.05	0	0.7071	0.7071	0.0708	0.0707
	1	0.4597	0.4347	-0.0623	-0.3701
	2	0.7671	-0.0915	13.1229	0.5654
	3	0.1552	2.6973	-166.4280	-6.6423
	4	-9.3017	-14.1195	1145.8217	45.7189
	5	97.3172	54.9653	-4762.0914	-189.9515
	6	-413.9673	-135.3432	12511.5152	498.8463
	7	936.4719	205.3051	-20927.0019	-834.5704
	8	-1078.2322	-173.3480	21613.9362	862.1672
	9	504.0555	62.8847	-12568.0268	-501.4354
	10			3148.4879	125.5869
0.1	0	0.7071	0.7072	0.1415	0.1414
	1	0.5498	0.5043	-0.1734	-0.3871
	2	1.5235	-0.5779	18.7434	1.2936
	3	-2.2395	7.6480	-266.7713	-17.0715
	4	-5.2844	-52.8793	2066.4692	132.0282
	5	226.0267	257.2074	-9661.5218	-617.3023
	6	-1423.2887	-799.7410	28556.2764	1826.3191
	7	4348.1446	1530.8314	-53734.1216	-3441.9797
	8	-6553.5540	-1634.0240	62435.9340	4007.6642
	9	3959.2116	749.0673	-40844.2364	-2628.6642
	10			11511.5912	743.3343
0.15	0	0.7071	0.7072	0.2122	0.2121
	1	0.7028	0.6376	-0.2929	-0.4042
	2	2.7653	-1.2331	26.3239	2.2494
	3	-7.2036	19.0057	-427.2558	-33.6757
	4	9.1384	-173.8407	3782.9591	297.4990
	5	667.4954	1108.9410	-20214.1250	-1590.1109
	6	-6105.7233	-4517.1019	68285.5344	5378.6049
	7	25260.2847	11317.3469	-146859.5866	-11588.2217
	8	-50586.0954	-15802.5485	195038.2341	15425.1699
	9	40325.8388	9475.7480	-145833.6228	-11566.8288
	10			46980.5243	3740.3538

Table 3 - cont.

d/h	i	b_{Ai}	b_{Bi}	c_{Ai}	c_{Bi}
0.20	0	0.7071	0.7072	0.2829	0.2828
	1	0.9394	0.8534	-0.4105	-0.4192
	2	5.0186	-2.2518	36.3675	3.4524
	3	-19.6345	47.2610	-686.9924	-59.3848
	4	76.1489	-589.3736	7097.1745	611.7194
	5	2376.8770	5125.5432	-44245.1037	-3814.7743
	6	-32402.0663	-28413.7181	174386.6733	15058.0019
	7	187563.3073	96818.0664	-437594.1661	-37860.2290
	8	-517758.7465	-183743.9141	678087.6506	58816.9514
	9	566112.6482	149736.5141	-591607.7634	-51479.6217
	10			222394.8277	19433.7456
0.25	0	0.7071	0.7071	0.3536	0.3536
	1	1.3041	1.1918	-0.5246	-0.4284
	2	9.6510	-4.1793	50.2589	4.8592
	3	-57.8163	129.7358	-1136.1027	-97.6558
	4	450.7761	-2325.3551	14085.0245	1206.5210
	5	10351.8621	29069.6053	-105370.0173	-9029.9162
	6	-227973.9193	-231101.0011	498386.1475	42788.3389
	7	1960136.6080	1128028.3541	-1500844.1305	-129153.3052
	8	-7899243.5583	-3063223.0225	2791092.0497	240895.9775
	9	12538854.7550	3568834.5097	-2922538.2779	-253169.5873
	10			1318591.9416	114779.2965
0.30	0	0.7071	0.7071	0.4244	0.4243
	1	1.9027	1.7480	-0.6553	-0.4321
	2	20.8636	-8.9087	72.3179	6.6403
	3	-197.8895	440.7103	-2037.1553	-160.0429
	4	2675.1513	-12390.9668	31569.7505	2468.7747
	5	71601.3880	241718.2677	-295202.5115	-23090.8486
	6	-2639273.5314	-2989605.6659	1745346.7908	136788.4159
	7	35994016.1511	22618755.1306	-6570139.7052	-516213.4074
	8	-227958779.2155	-94950523.9757	15273818.2302	1203928.2026
	9	567162515.8604	170542044.2578	-19993047.6604	-1582260.0614
	10			11276922.9053	897240.7983

Table 4. The stress intensity factor and the coefficients of the shape function for a strip with two collinear symmetric edge cracks of depths L/2 under tension σ.

L/h	$K_1/\sigma\sqrt{\pi L/2}$	b_i	i
0.0001	1.1221	0.7934	0
0.1	1.1231	0.0775	1
0.2	1.1254	-0.7542	2
0.3	1.1292	7.5825	3
0.4	1.1370	-12.1712	4
0.5	1.1546	-186.5011	5
0.6	1.2117	1236.2858	6
0.7	1.3254	-3043.6190	7
0.8	1.5393	3350.3456	8
0.9	2.0836	-1374.8426	9

Table 5. Normalized stress intensity factor K/K_0 calculated at the midsection of two opposite planar elliptic surface cracks in a plate under uniform tension σ_0, $K_0=\sigma_0\sqrt{\pi L_0/2}$ (Fig. 4).

L_0/h \ a/L_0 →	1.0	2.0	3.0	4.0	10.0	100.0	Plane Strain
0.1	1.060	1.089	1.099	1.104	1.113	1.119	1.123
0.2	1.009	1.062	1.081	1.091	1.109	1.121	1.125
0.3	0.966	1.028	1.065	1.079	1.106	1.124	1.129
0.4	0.929	1.019	1.053	1.072	1.108	1.131	1.137
0.5	0.902	1.008	1.050	1.073	1.118	1.148	1.155
0.6	0.902	1.038	1.080	1.108	1.165	1.203	1.212
0.7	0.929	1.082	1.149	1.186	1.262	1.315	1.325
0.8	0.997	1.195	1.284	1.336	1.445	1.524	1.539

Table 6. Maximum normalized stress intensity factor K/K_0 for two planar elliptic surface cracks in a plate under uniform tension σ_0, $K_0=\sigma_0\sqrt{\pi L_0}$. (Fig. 5a, d=h/2) d=h/2

L_0/h	a/L_0 \ b/a	0.1	1.0	4.0	20.0	Single Crack
0.1	2	0.996	0.986	0.982	0.981	0.981
0.1	4	1.072	1.065	1.062	1.062	1.062
0.1	10	1.127	1.122	1.121	1.120	1.120
0.2	2	0.979	0.959	0.951	0.949	0.949
0.2	4	1.107	1.090	1.084	1.082	1.082
0.2	10	1.221	1.210	1.207	1.206	1.206
0.3	2	1.007	0.975	0.963	0.961	0.961
0.3	4	1.189	1.160	1.151	1.149	1.149
0.3	10	1.382	1.364	1.359	1.358	1.358
0.4	2	1.051	1.006	0.991	0.989	0.989
0.4	4	1.299	1.255	1.243	1.240	1.240
0.4	10	1.600	1.571	1.563	1.562	1.562
0.5	2	1.106	1.048	1.032	1.030	1.030
0.5	4	1.430	1.370	1.354	1.352	1.352
0.5	10	1.879	1.836	1.824	1.822	1.821
0.6	2	1.230	1.096	1.080	1.077	1.077
0.6	4	1.568	1.491	1.472	1.469	1.469
0.6	10	2.208	2.141	2.124	2.121	2.121
0.7	2	1.370	1.120	1.100	1.097	1.097
0.7	4	1.694	1.575	1.553	1.550	1.550
0.7	10	2.532	2.434	2.409	2.405	2.405

Table 7. Maximum normalized stress intensity factor K/K_0 for two planar elliptic surface cracks in a plate under uniform bending M, $K_0=\sigma_b\sqrt{\pi L_0}$, $\sigma_b=6M/h^2$ (Fig. 5a, d=h/2).

L_0/h	a/L_0	b/a → 0.1	1.0	4.0	20.0	Single Crack
0.1	2	0.874	0.864	0.861	0.860	0.860
0.1	4	0.943	0.936	0.934	0.933	0.933
0.1	10	0.992	0.988	0.987	0.986	0.986
0.2	2	0.766	0.728	0.719	0.718	0.718
0.2	4	0.847	0.830	0.825	0.824	0.824
0.2	10	0.940	0.930	0.927	0.927	0.927
0.3	2	0.751	0.665	0.651	0.650	0.650
0.3	4	0.803	0.755	0.745	0.744	0.744
0.3	10	0.915	0.900	0.896	0.896	0.895
0.4	2	0.792	0.677	0.659	0.658	0.656
0.4	4	0.801	0.726	0.713	0.711	0.711
0.4	10	0.923	0.902	0.896	0.895	0.895
0.5	2	0.826	0.684	0.663	0.661	0.659
0.5	4	0.834	0.719	0.703	0.701	0.700
0.5	10	0.950	0.910	0.902	0.901	0.901
0.6	2	0.855	0.686	0.662	0.660	0.659
0.6	4	0.909	0.743	0.724	0.722	0.721
0.6	10	0.995	0.925	0.912	0.910	0.910
0.7	2	0.874	0.683	0.658	0.655	0.654
0.7	4	0.989	0.784	0.761	0.759	0.757
0.7	10	1.064	0.956	0.939	0.937	0.936

Table 8. Normalized stress intensity factor K/K_o calculated at the midsection of symmetrically located (d=0) two identical planar internal elliptic cracks in a plate under uniform tension σ_o, $K_o=\sigma_o\sqrt{\pi L_o/2}$ (Fig. 5a).

L_o/h	a/L_o	b/a → 0.1	1.0	4.0	20.0	Single Crack
0.1	2	0.977	0.976	0.976	0.976	0.976
0.1	4	0.987	0.987	0.987	0.986	0.987
0.1	10	0.994	0.993	0.993	0.993	0.993
0.2	2	0.975	0.972	0.971	0.971	0.971
0.2	4	0.995	0.994	0.993	0.993	0.993
0.2	10	1.008	1.007	1.007	1.007	1.007
0.3	2	0.980	0.980	0.979	0.979	0.979
0.3	4	1.015	1.013	1.012	1.012	1.012
0.3	10	1.035	1.034	1.034	1.034	1.034
0.4	2	1.007	1.002	1.000	1.000	1.000
0.4	4	1.051	1.048	1.047	1.047	1.047
0.4	10	1.080	1.078	1.078	1.078	1.078
0.5	2	1.046	1.039	1.037	1.036	1.036
0.5	4	1.106	1.102	1.101	1.101	1.101
0.5	10	1.147	1.145	1.145	1.145	1.145
0.6	2	1.108	1.098	1.095	1.095	1.095
0.6	4	1.190	1.185	1.183	1.183	1.183
0.6	10	1.248	1.246	1.245	1.245	1.245
0.7	2	1.205	1.192	1.188	1.187	1.187
0.7	4	1.321	1.313	1.311	1.310	1.310
0.7	10	1.407	1.404	1.403	1.403	1.403
0.8	2	1.367	1.348	1.342	1.341	1.341
0.8	4	1.541	1.529	1.526	1.525	1.525
0.8	10	1.681	1.676	1.674	1.674	1.674
0.9	2	1.703	1.672	1.662	1.661	1.661
0.9	4	2.007	1.988	1.982	1.981	1.981
0.9	10	2.285	2.275	2.272	2.272	

Table 9. Normalized stress intensity factors K_A/K_o and K_B/K_o calculated at the midsection of three identical planar internal elliptic cracks in a plate under uniform tension σ_o, $K_o=\sigma_o\sqrt{\pi L_o/2}$.

The middle crack

	d	L_o/h	a/L_o	b/a → 0.1	1.0	4.0	20.0
$\frac{K_A}{K_o}$	0.1	0.1	2	0.983	0.981	0.979	0.979
	0.1	0.1	4	0.994	0.992	0.992	0.991
	0.1	0.2	2	0.985	0.980	0.977	0.976
	0.1	0.2	4	1.007	1.004	1.002	1.001
	0.1	0.3	2	1.006	0.997	0.991	0.989
	0.1	0.3	4	1.040	1.035	1.032	1.031
	0.2	0.1	2	0.981	0.978	0.976	0.975
	0.2	0.1	4	0.995	0.994	0.992	0.992
	0.2	0.2	2	0.993	0.986	0.981	0.979
	0.2	0.2	4	1.023	1.018	1.015	1.014
	0.3	0.1	2	0.983	0.979	0.976	0.975
	0.3	0.1	4	1.003	1.001	0.999	0.998
$\frac{K_B}{K_o}$	0.1	0.1	2	0.983	0.981	0.979	0.979
	0.1	0.1	4	0.994	0.992	0.991	0.991
	0.1	0.2	2	0.984	0.980	0.977	0.976
	0.1	0.2	4	1.003	1.001	0.999	0.999
	0.1	0.3	2	0.997	0.990	0.986	0.984
	0.1	0.3	4	1.026	1.022	1.020	1.019
	0.2	0.1	2	0.981	0.978	0.976	0.975
	0.2	0.1	4	0.994	0.993	0.992	0.991
	0.2	0.2	2	0.987	0.981	0.977	0.976
	0.2	0.2	4	1.012	1.009	1.006	1.005
	0.3	0.1	2	0.981	0.977	0.975	0.974
	0.3	0.1	4	0.999	0.997	0.996	0.995

Table 9 - Cont.

The outer cracks

	d	L_o/h	a/L_o	b/a → 0.1	1.0	4.0	20.0
$\frac{K_A}{K_o}$	0.1	0.1	2	0.982	0.980	0.979	0.979
	0.1	0.1	4	0.993	0.992	0.991	0.991
	0.1	0.2	2	0.982	0.978	0.976	0.976
	0.1	0.2	4	1.005	1.003	1.002	1.001
	0.1	0.3	2	0.999	0.994	0.991	0.989
	0.1	0.3	4	1.037	1.034	1.032	1.031
	0.2	0.1	2	0.979	0.977	0.976	0.975
	0.2	0.1	4	0.994	0.993	0.992	0.992
	0.2	0.2	2	0.988	0.983	0.980	0.979
	0.2	0.2	4	1.019	1.016	1.014	1.014
	0.3	0.1	2	0.980	0.978	0.976	0.975
	0.3	0.1	4	1.001	1.000	0.999	0.998
$\frac{K_B}{K_o}$	0.1	0.1	2	0.982	0.980	0.979	0.979
	0.1	0.1	4	0.993	0.992	0.991	0.991
	0.1	0.2	2	0.981	0.978	0.976	0.976
	0.1	0.2	4	1.002	1.000	0.999	0.999
	0.1	0.3	2	0.992	0.988	0.985	0.984
	0.1	0.3	4	1.023	1.021	1.020	1.019
	0.2	0.1	2	0.979	0.978	0.976	0.975
	0.2	0.1	4	0.993	0.992	0.991	0.991
	0.2	0.2	2	0.983	0.979	0.977	0.976
	0.2	0.2	4	1.010	1.007	1.006	1.005
	0.3	0.1	2	0.978	0.976	0.974	0.974
	0.3	0.1	4	0.998	0.996	0.995	0.995

Table 10. Normalized stress intensity factors on the crack front for an internal elliptic crack in a plate under uniform membrane load $N_{22}=h\sigma_o$ and bending moment $M_{22}=h^2\sigma_b/h$ with $d/h=0.20$, $L_o/h=0.45$, $a/L_o=4$, $K=\sigma_o\sqrt{\pi L_o/2}$ or $K_o=\sigma_b\sqrt{\pi L_o/2}$ (see Fig. 3).

x_1/a	$(K_A/K_o)_N$	$(K_B/K_o)_N$	$(K_B/K_o)_M$	$(K_B/K_o)_M$
0.90	0.723	0.707	0.357	0.218
0.80	0.865	0.831	0.454	0.229
0.70	0.974	0.916	0.531	0.233
0.60	1.065	0.980	0.595	0.233
0.50	1.143	1.028	0.649	0.233
0.40	1.211	1.068	0.697	0.233
0.30	1.266	1.096	0.735	0.233
0.20	1.307	1.116	0.763	0.233
0.10	1.333	1.128	0.781	0.233
0.00	1.342	1.132	0.787	0.232

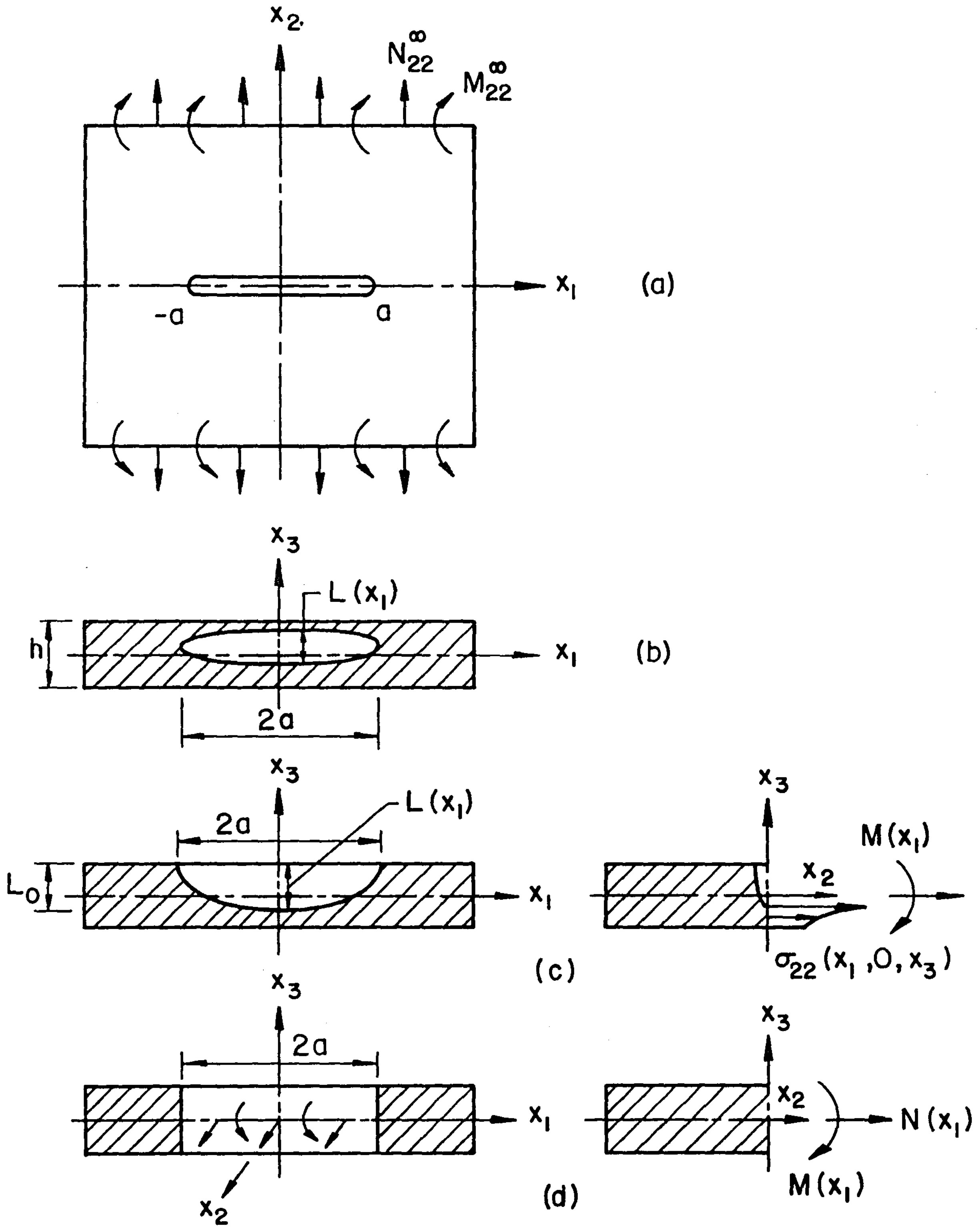

Fig. 1 Notation for internal and surface cracks

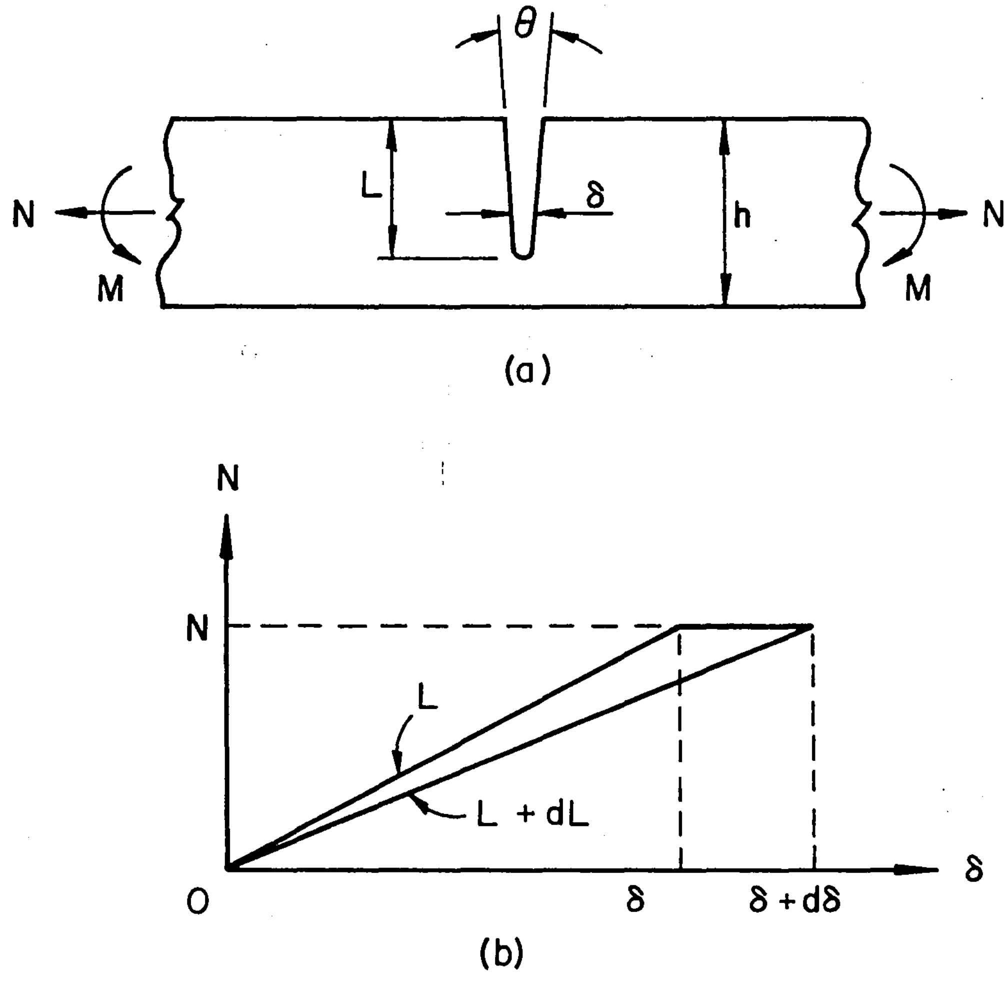

Fig. 2 The corresponding plane strain problem

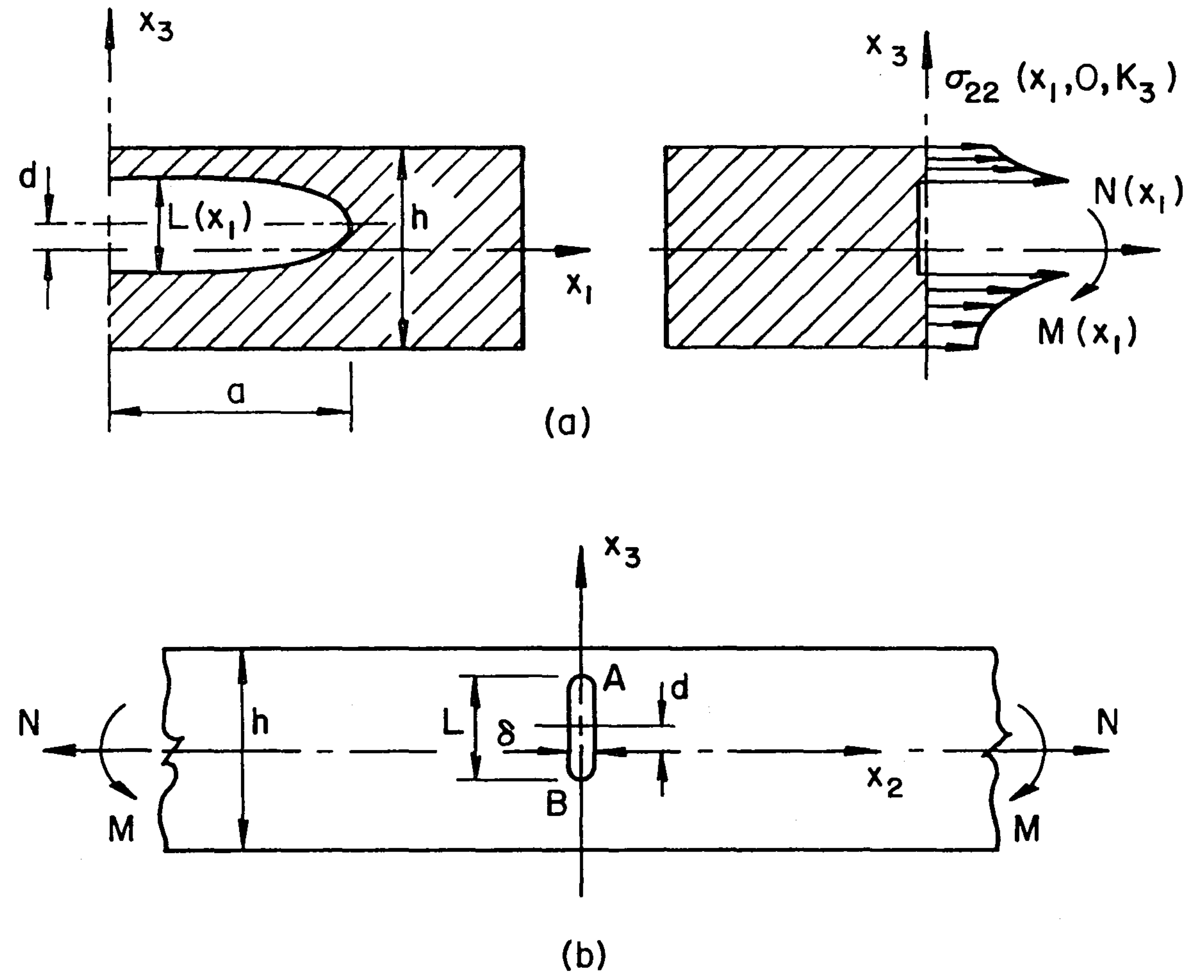

Fig. 3 Notation for an internal part-through crack

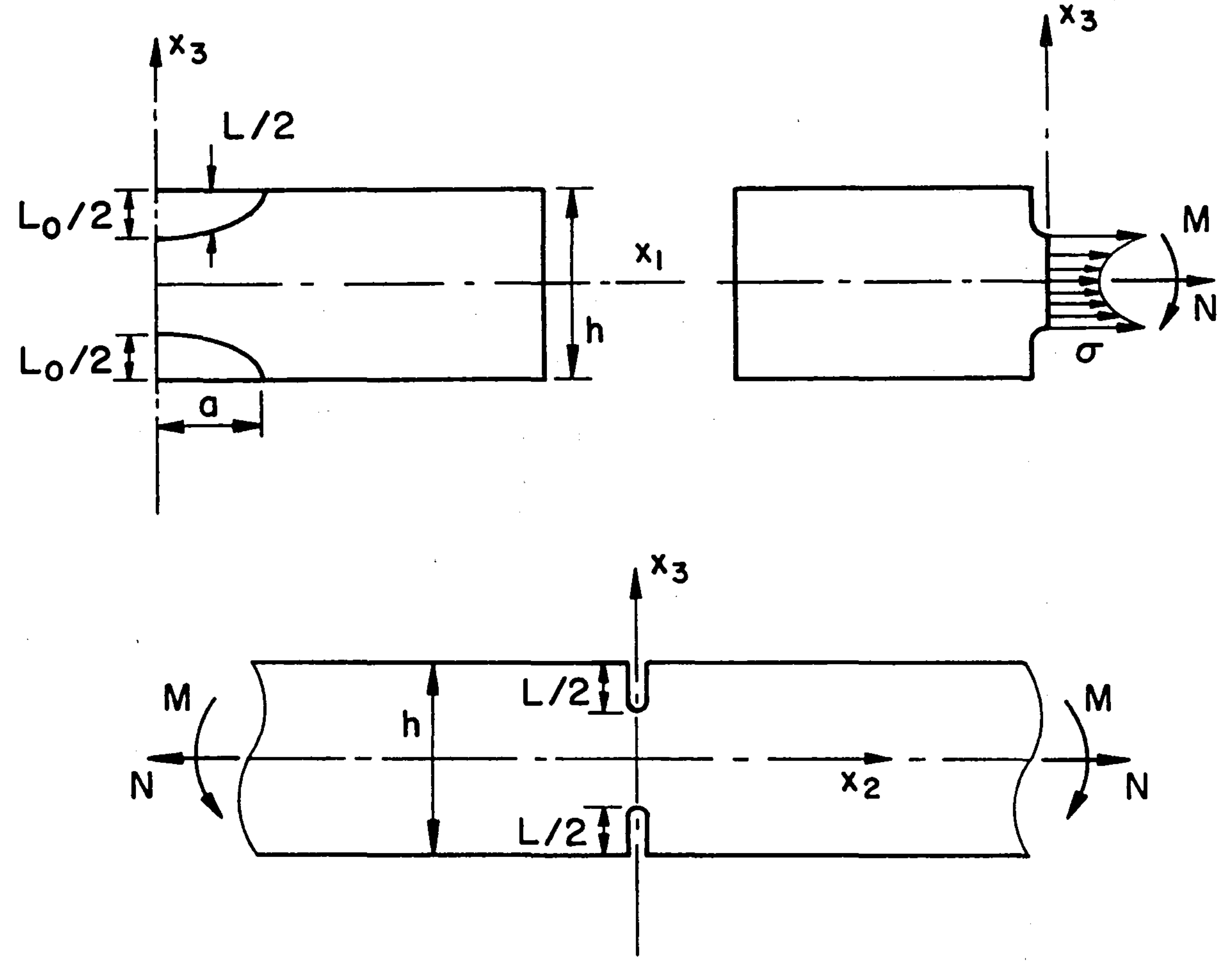

Fig. 4 Geometry and notation for two coplanar semi-elliptic surface cracks on the opposite sides of the plate

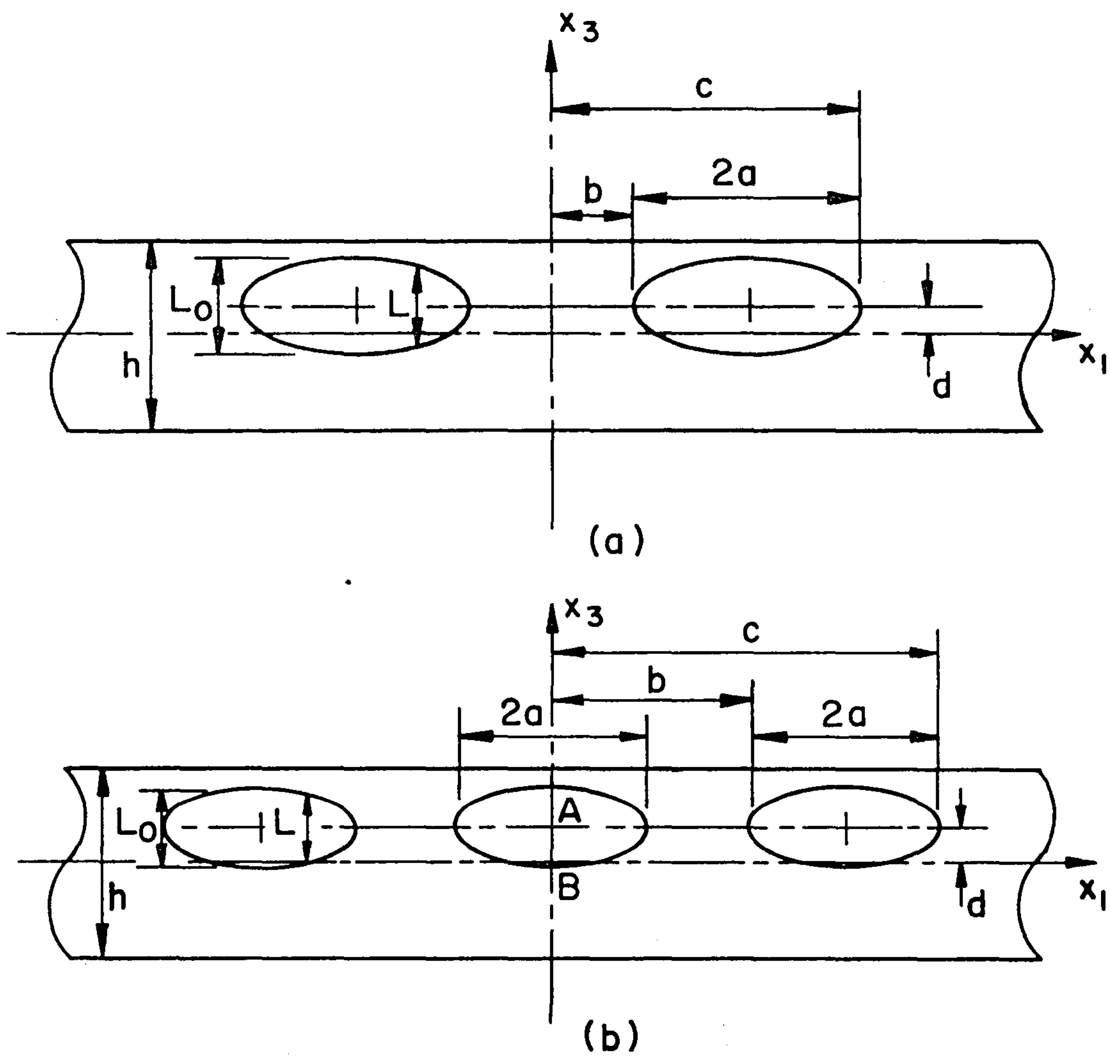

Fig. 5 Geometry and notation for coplanar internal elliptic cracks

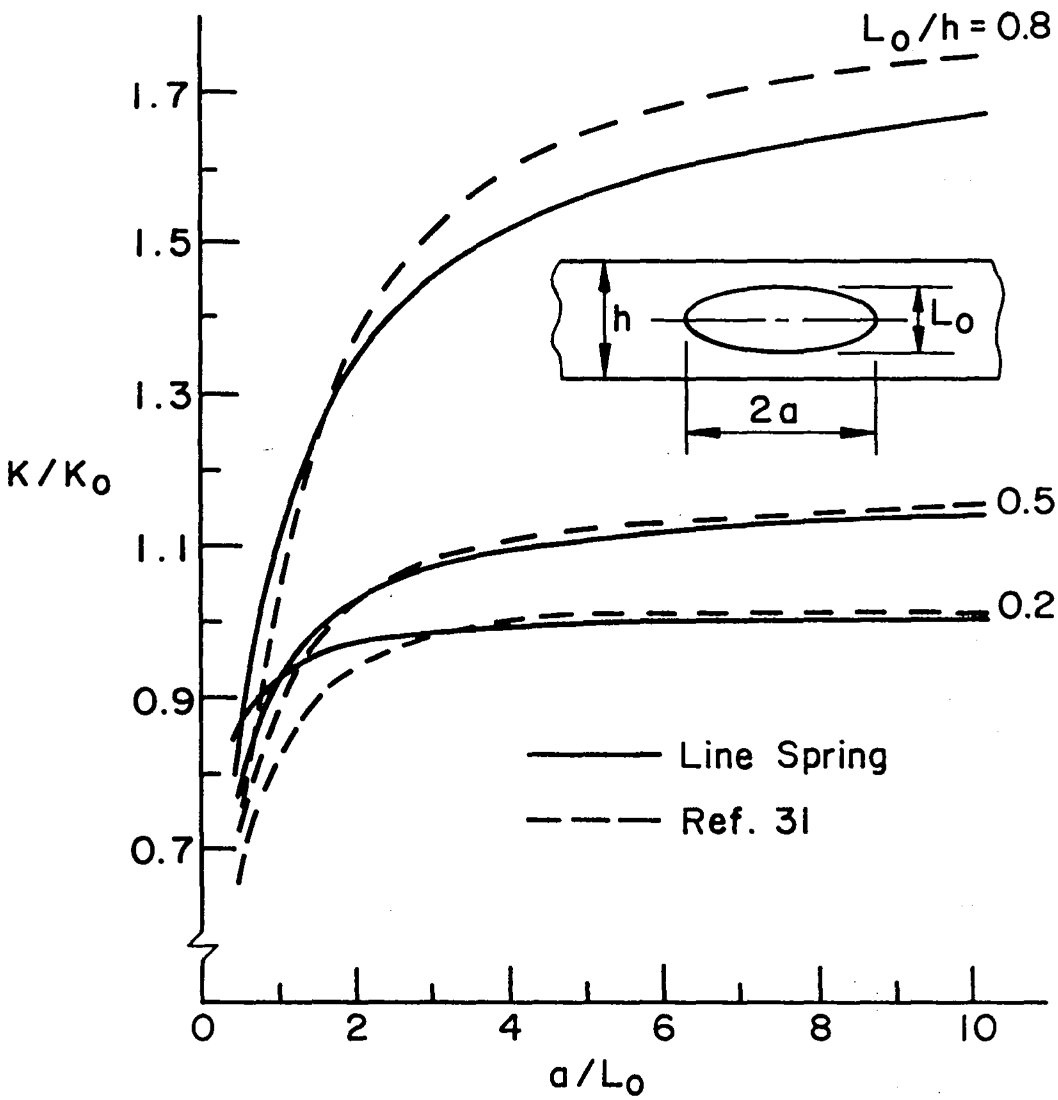

Fig. 6 Normalized stress intensity factor for a symmetrically located internal elliptic crack (d=0, Fig. 3) in a plate under uniform tension perpendicular to the crack plane, $K_o = \sigma_o\sqrt{\pi L_o/2}$

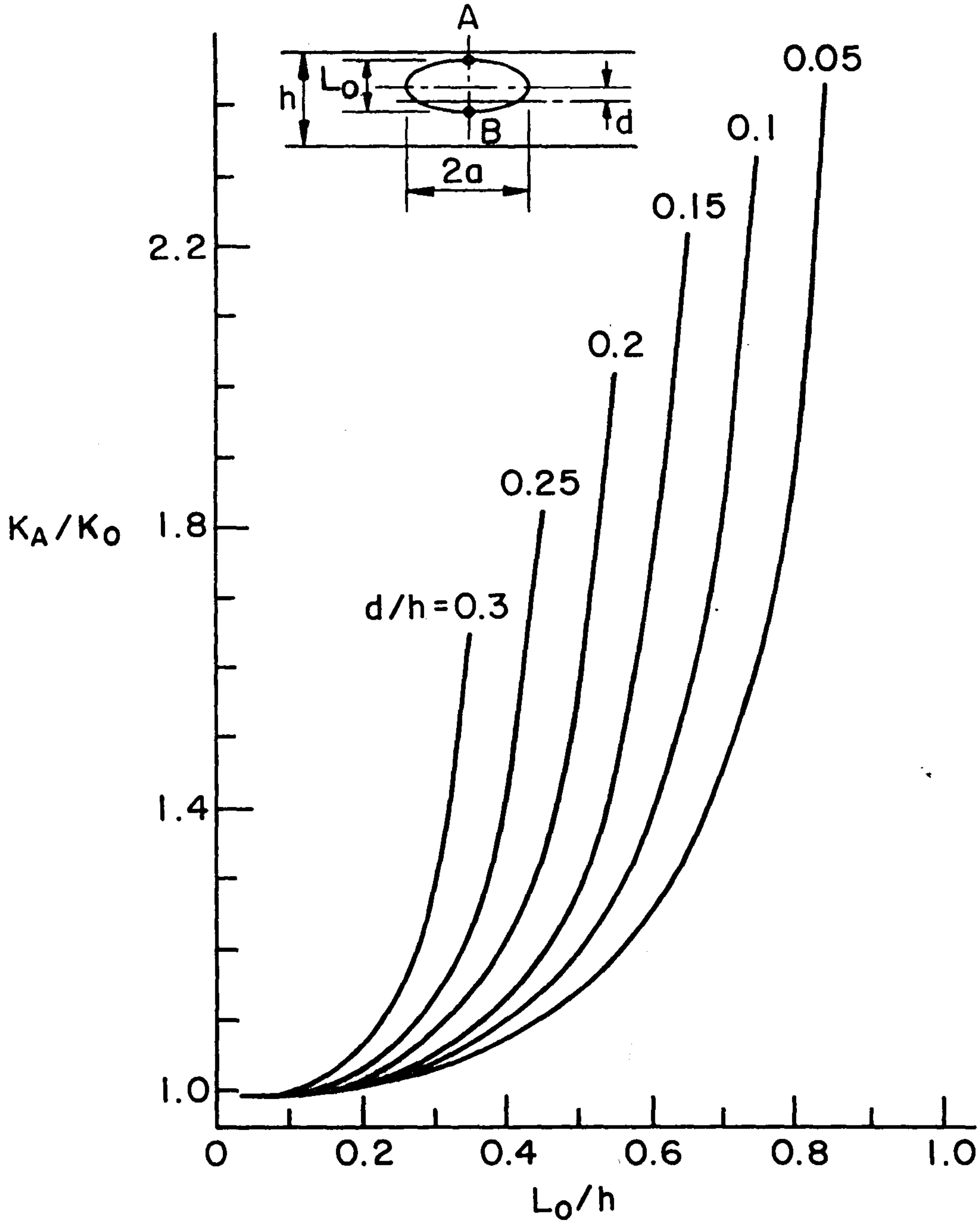

Fig. 7 Normalized stress intensity factor at the midsection of an eccentrically located internal elliptic crack in a plate under uniform tension σ_0 ($a/L_0=4$, $K_0=\sigma_0\sqrt{\pi L_0/2}$, subscript A refers to the smaller net ligament).

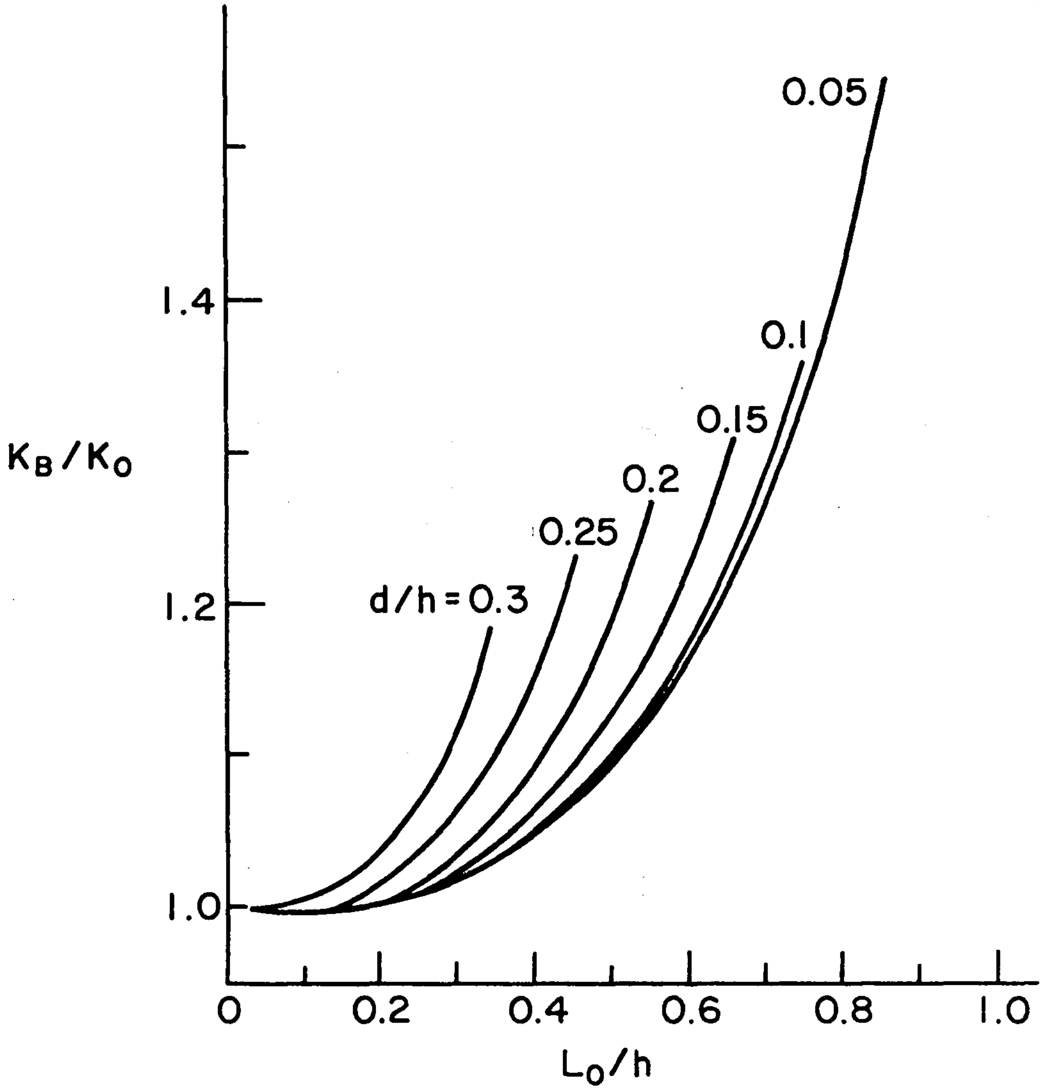

Fig. 8 Same as Fig. 7 (subscript B refers to the greater net ligament)

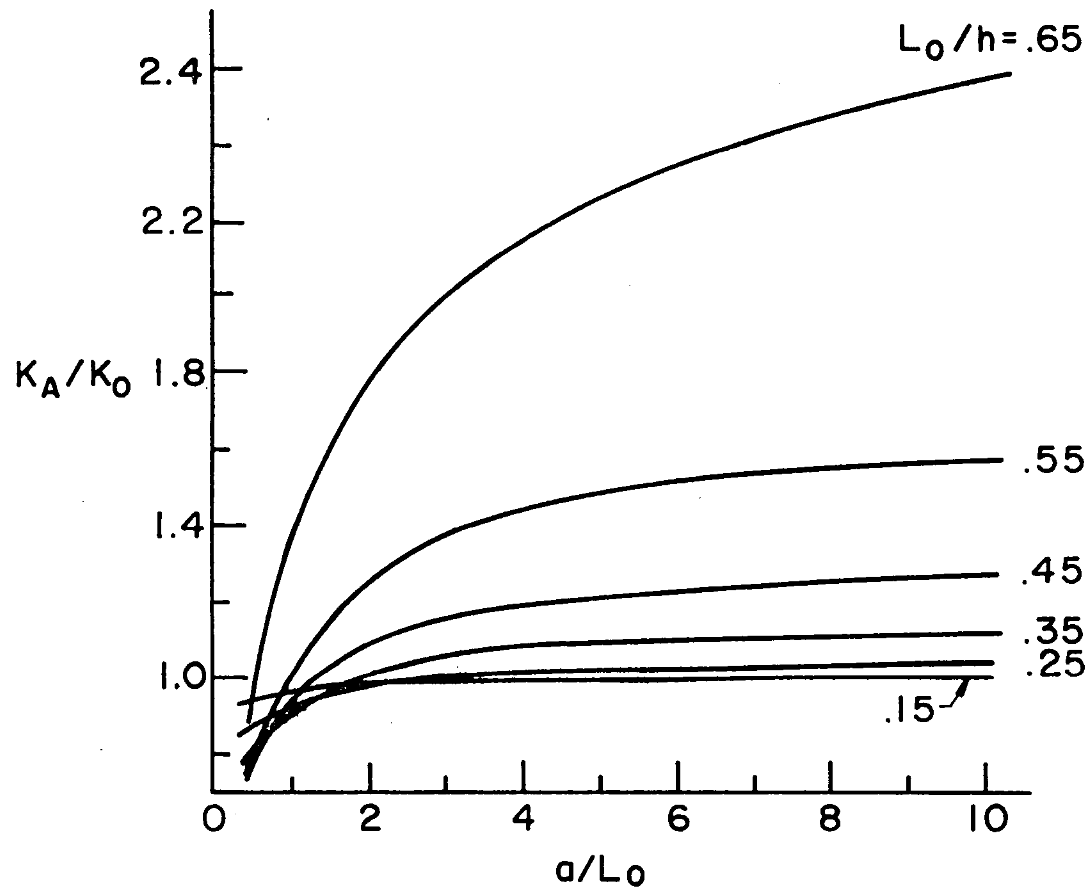

Fig. 9 Normalized stress intensity factor at the midsection of an eccentrically located internal elliptic crack in a plate under tension σ_0 ($d/h=0.15$, $K_0=\sigma_0\sqrt{\pi L_0/2}$, see insert in Fig. 7).

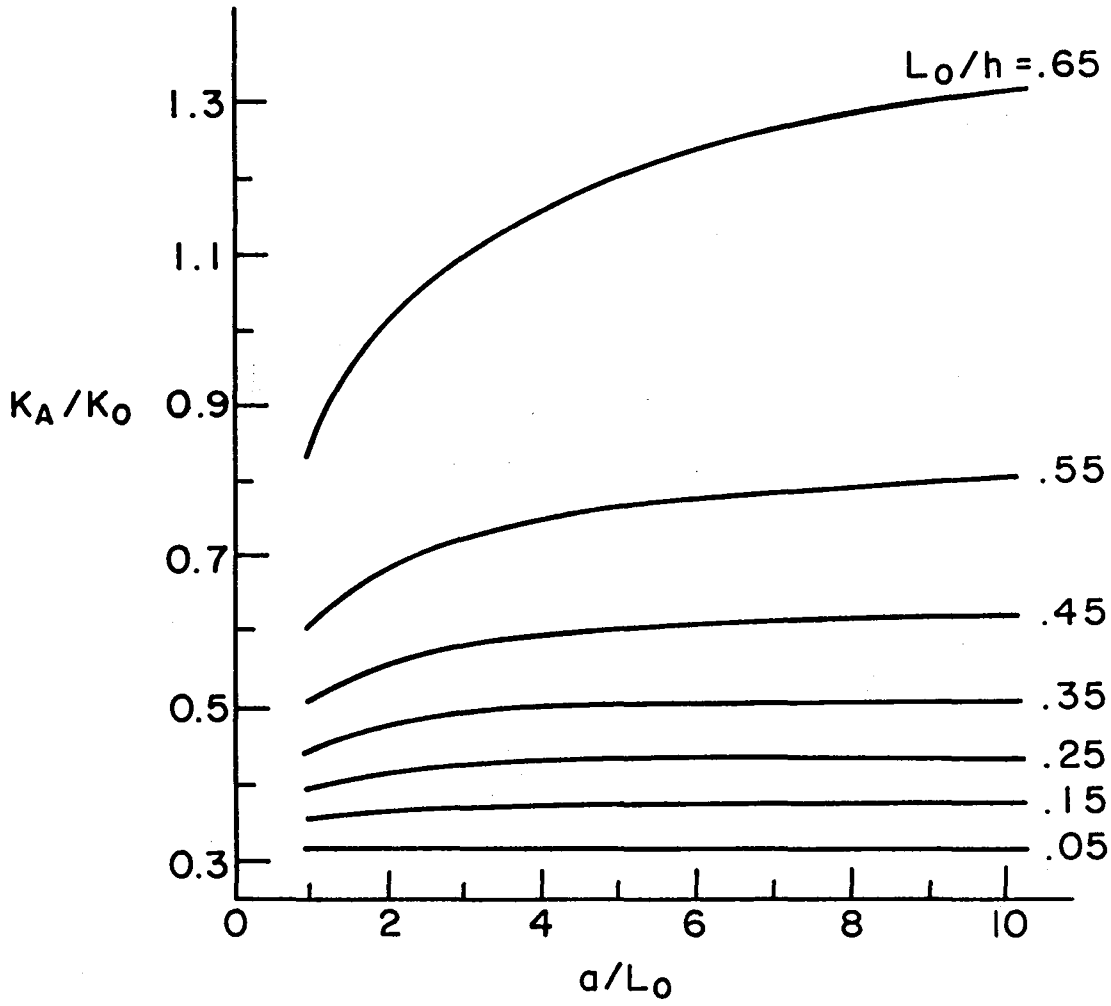

Fig. 10 Same as in Fig. 9, stress intensity factor for the greater net ligament

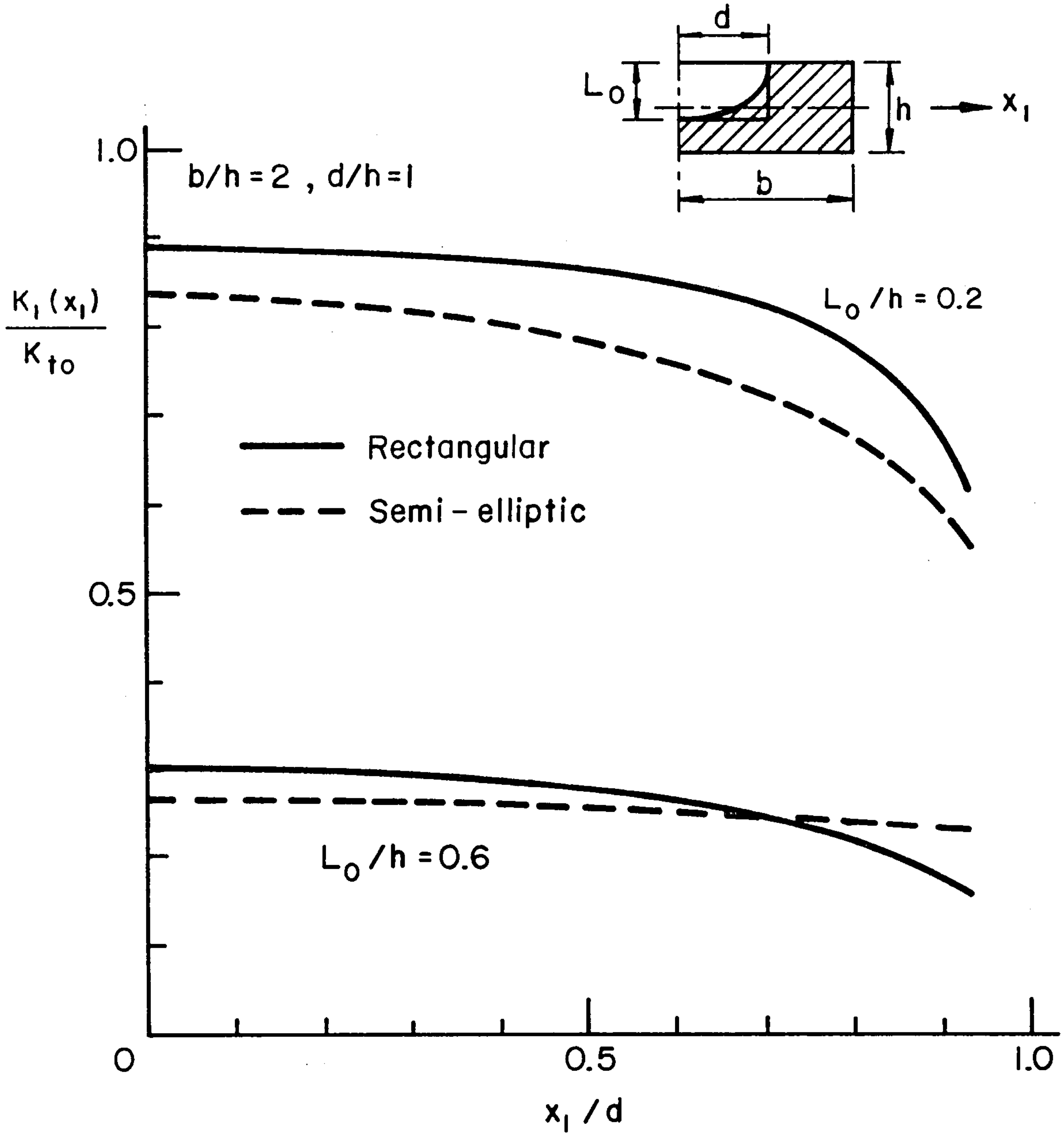

Fig. 11 Distribution of the normalized stress intensity factor along the front of a semi-elliptic and a rectangular surface crack in a plate of finite width under uniform tension perpendicular to the crack plane

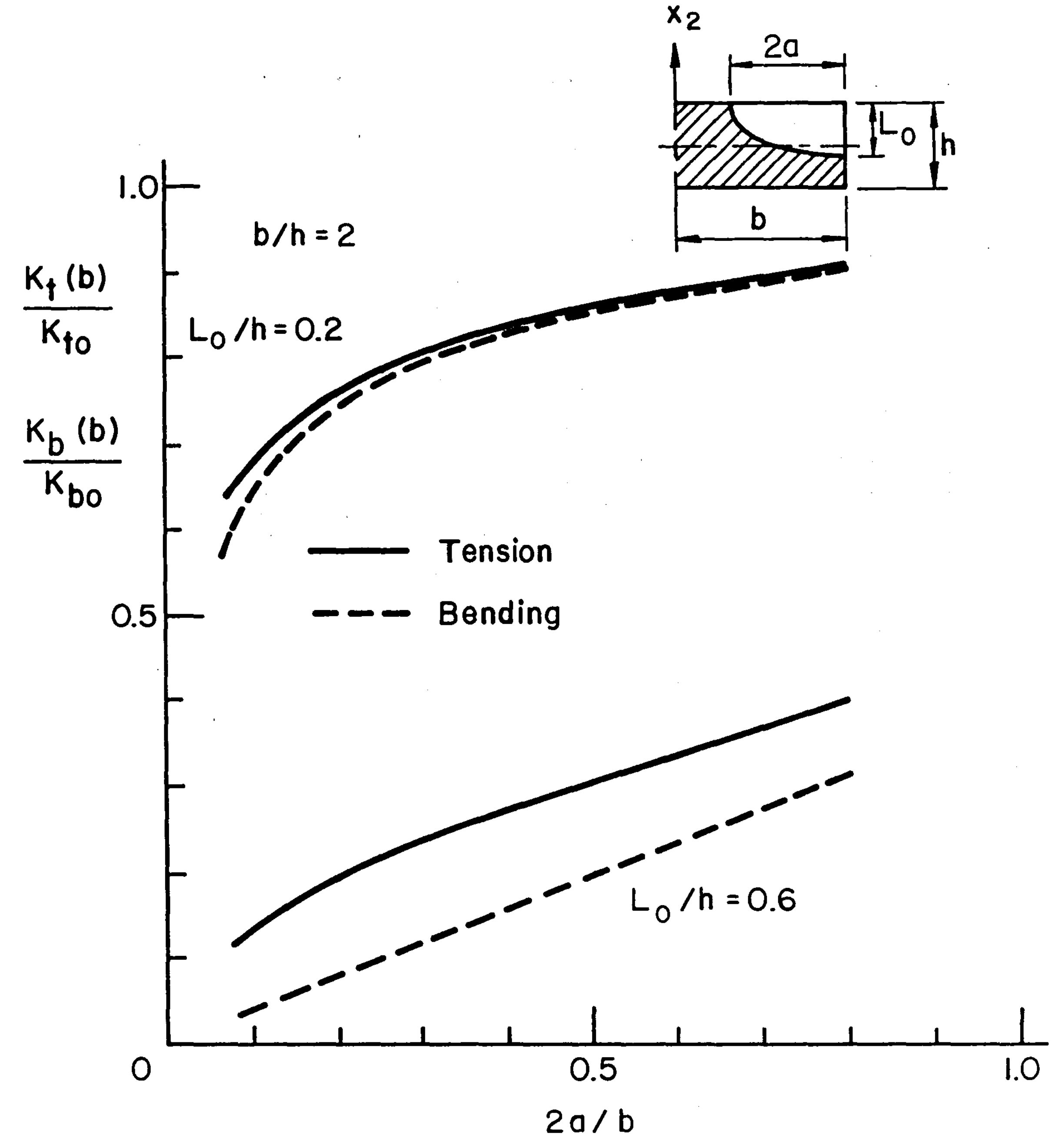

Fig. 12 Stress intensity factor at the maximum penetration point of elliptic corner cracks in a plate of finite width under tension and bending

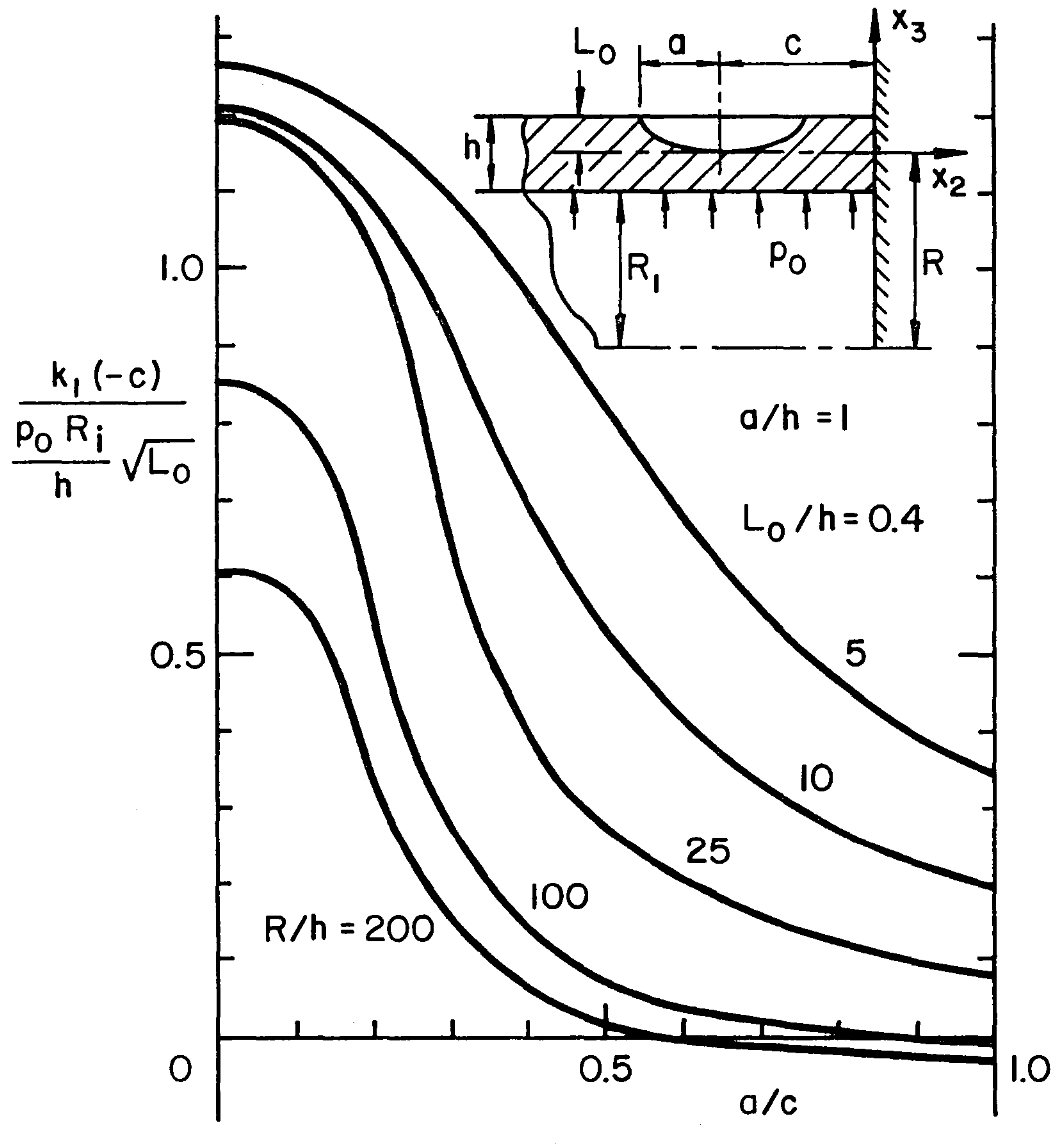

Fig. 13 Stress intensity factor at the midsection of a semi-elliptic axial surface crack in a pressurized cylinder with a fixed end (ν=0.3, a/h=1, L_0/h=0.4)

Standard Bibliographic Page

1. Report No.	2. Government Accession No.	3. Recipient's Catalog No.
NASA CR-178141		

4. Title and Subtitle	5. Report Date
Line Spring Model And Its Applications To Part-Through Crack Problems In Plates And Shells	June 1986
	6. Performing Organization Code
7. Author(s) F. Erdogan and B. Aksel	8. Performing Organization Report No.
9. Performing Organization Name and Address Lehigh University Bethlehem, Pennsylvania 18015	10. Work Unit No.
	11. Contract or Grant No. NGR 39-007-011
12. Sponsoring Agency Name and Address National Aeronautics and Space Administration Washington, DC 20546	13. Type of Report and Period Covered Contractor Report
	14. Sponsoring Agency Code 506-43-11-04

15. Supplementary Notes

Langley Technical Monitor: Dr. C. A. Bigelow

16. Abstract

In this paper a general description of the line spring model is presented. It is then extended to cover the problem of interaction of multiple internal and surface cracks in plates and shells. The shape functions for various related crack geometries obtained from the plane strain solution and the results of some multiple crack problems are presented. The problems considered include coplanar surface cracks on the same or opposite sides of a plate, nonsymmetrically located coplanar internal elliptic cracks, and in a very limited way the surface and corner cracks in a plate of finite width and a surface in a cylindrical shell with fixed end.

17. Key Words (Suggested by Authors(s))	18. Distribution Statement
Stress intensity factor cracks in plates Line spring model cracks in shells Surface crack Internal crack Three dimensional crack problem Part-Through crack	Unclassified-Unlimited Subject Category 39

19. Security Classif.(of this report)	20. Security Classif.(of this page)	21. No. of Pages	22. Price
Unclassified	Unclassified	43	A03

For sale by the National Technical Information Service, Springfield, Virginia 22161

NASA Langley Form 63 (June 1985)

End of Document